

St. John's University

St. John's Scholar

Theses and Dissertations

2024

PRODUCTION OF VP3-ONLY AAV2 VLP IN E. COLI

Chengyu Fu

Follow this and additional works at: https://scholar.stjohns.edu/theses_dissertations



Part of the [Pharmacology Commons](#)

PRODUCTION OF VP3-ONLY AAV2 VLP IN E. COLI

A dissertation submitted in partial fulfillment
of the requirements for the degree of

DOCTOR OF PHILOSOPHY

to the faculty of the

DEPARTMENT OF PHARMACEUTICAL SCIENCES

of

COLLEGE OF PHARMACY AND HEALTH SCIENCES

at

ST. JOHN'S UNIVERSITY

New York

by

Chengyu Fu

Date Submitted 12/10/2023

Date Approved 12/14/2023

Chengyu Fu

Dr. Woon-Kai Low

© Copyright by Chengyu Fu 2024

All Rights Reserved

ABSTRACT

PRODUCTION OF VP3-ONLY AAV2 VLP IN *E. COLI*

Chengyu Fu

Adeno-associated virus (AAV) is a widely used vector for gene therapy. However, few studies have focused on producing AAV-based virus-like particles (VLP) in *E. coli*. This project aimed to express VP3 of AAV2 or co-express VP3 of AAV2 with other proteins, such as *E. coli* chaperones and/or assembly-activating protein (AAP) in *E. coli* under different expression conditions and explore the potential to produce VP3-only VLP of AAV2 *in situ* in *E. coli*.

The constructed plasmid pET15ΔHis-VP3 was used to express VP3 under different conditions. The results demonstrated that most expressed VP3 was in inclusion bodies in all tested conditions. Although low level of soluble VP3 could be produced in *E. coli* after optimization, those proteins might be present as monomers or aggregates. To promote the assembly of VP3, the constructed plasmid pET15ΔHis-VP3-AAP was used to co-express VP3 and AAP in *E. coli*. Assembled VP3-only VLP could be detected with dot blot assays and transmission electron microscopy after co-expression at 30 °C. However, the overall production level of VP3 after co-expression was lower than that after expression of VP3 alone. Therefore, we tried co-expression VP3 with *E. coli* chaperones (trigger factor, Hsp70 and chaperonin) instead of AAP. It showed that those chaperones were able to facilitate soluble expression of VP3 and prevent its aggregation, but only Hsp70 and

chaperonin had small effects on promoting VP3-only VLP assembly. Triple co-expression of VP3, AAP and chaperones using *E. coli* (BL21 (DE3)) demonstrated that chaperonin could increase the production of VP3-only VLP when triple co-expressing VP3, AAP and chaperonin.

Purification of VP3-only VLP of AAV2 was also attempted. Although partial purification could be achieved with polyethylenimine (PEI) precipitation followed by size exclusion chromatography with Sephacryl S-300 HR, further purification was hampered by the low yields.

In conclusion, our results demonstrated that the *in situ* production of VP3-only VLP of AAV2 in *E. coli* was possible. However, further optimizations of expression conditions as well as purification conditions may be necessary to achieve a high yield of produced VLP.

ACKNOWLEDGEMENTS

First, I would like to extend my deepest gratitude to my mentor, Dr. Low, for his invaluable patience, guidance, and insightful feedback throughout my doctoral journey. I am truly grateful for the privilege of having learned and thrived under his mentorship.

To the members of my defense committee, Dr. Kunda, Dr. Martino, Dr. Trombetta, Dr. Wurpel, and chair of the defense, Dr. Muth, I offer my sincere appreciation for their time, expertise, and thoughtful critiques. Their insightful questions and suggestions significantly strengthened my research and contributed to the quality of this dissertation.

I am also grateful to Dr. Kolipara, Susana Solis, Velda Glover and other professors or faculties in the Department of Pharmaceutical Sciences who support me in my class or TA work.

Further, I would like to thank Dr. Gupta and Dr. Gillespie, who help me in my course registration.

To my fellow lab mates and friends, Eason, Ganming, Jason, Joseph, Shilpa, Shruthi, Sisi, Twist, Vera, Xiaoxiao, Xingduo and Yidong, I appreciate their help and encouragement in my daily lives.

Lastly, I would like to express my deepest gratitude to my parents for their constant support throughout this challenging yet rewarding process. I would not be here without their love and support.

TABLE OF CONTENTS

ACKNOWLEDGEMENTS	ii
LIST OF TABLES	ix
LIST OF FIGURES	x
LIST OF ABBREVIATIONS	xi
CHAPTER 1 INTRODUCTION	1
1.1. Virus-like particles (VLPs)	1
1.1.1. Expression and purification of VLPs	1
1.1.1.1. Expression of VLPs	1
1.1.1.2. Purification of VLPs	2
1.1.2. Characterization of VLPs	5
1.1.3. Application of VLPs	6
1.2. Adeno-associated virus (AAV)	10
1.2.1. Genome of AAV	10
1.2.2. Capsids of AAV	15
1.2.2.1. Capsid structures of AAV	15
1.2.2.2. Capsid assembly of AAV	16
1.2.3. Production of recombinant AAV (rAAV) and AAV-based VLPs	18
1.2.4. Purification of rAAV	21

1.2.4.1. Density gradient ultracentrifugation.....	21
1.2.4.2. Hydrophobic Interaction Chromatography	24
1.2.4.3. Ion Exchange Chromatography	25
1.2.4.4. Size Exclusion Chromatography	26
1.2.4.5. Heparin Affinity Chromatography	27
1.2.4.6. Immunoaffinity Chromatography.....	28
1.3. Chaperones and protein folding in E. coli	28
1.4. Goal of the study.....	31
1.4.1. Hypothesis.....	31
1.4.2. Objective	31
1.4.3. Specific aims	31
CHAPTER 2 MATERIALS AND METHODS	33
2.1. Materials	33
2.1.1. Regents for bacterial culture and protein expression.....	33
2.1.2. Molecular cloning reagents.....	33
2.1.3. Plasmids and vectors.....	34
2.1.4. Antibodies	34
2.1.5. Primers and oligos.....	34
2.1.6. Other reagents and materials.....	36
2.2. Buffers and solutions	38

2.3. Methods.....	41
2.3.1. Plasmid construction.....	41
2.3.1.1. DNA mini-prep plasmid preparation and DNA sequencing	41
2.3.1.2. Construction of pET15b- Δ His.....	41
2.3.1.3. PCR amplification of AAV2VP3, AAV2AAP and T7-AAV2AAP	42
2.3.1.4. Construction of pET15b- Δ His-VP3 and pET15b-AAP	42
2.3.1.5. SLiCE extract preparation	45
2.3.1.6. Construction of pET15b- Δ His-VP3-AAP	45
2.3.2. Recombinant protein expression in <i>E. coli</i>	46
2.3.2.1. Traditional IPTG-based induction of recombinant VP3 expression	46
2.3.2.2. Auto-induction of recombinant VP3 using ZYP-5052.....	47
2.3.2.3. Auto-induction of recombinant VP3 with or without other proteins using LB-505	48
2.3.3. Cell lysis.....	51
2.3.3.1. Cell lysis protocol 1 (small-scale expression).....	51
2.3.3.2. Cell lysis protocol 2 (larger-scale expression)	51
2.3.4. SDS-PAGE	52
2.3.4.1. Sample preparation and electrophoresis.....	52
2.3.4.2. Polyacrylamide gel staining	53
2.3.5. Western blot.....	53
2.3.6. Dot blot	54

2.3.7.	Iodixanol gradient ultracentrifugation	55
2.3.8.	PEG precipitation.....	56
2.3.9.	Triton X-114 phase separation.....	56
2.3.10.	Polyethylenimine (PEI) protein precipitation	57
2.3.11.	Ammonium sulfate protein precipitation	57
2.3.12.	Protein purification by chromatography	58
2.3.13.	Transmission electron microscopy	58
CHAPTER 3 RESULTS.....		61
3.1.	AAP promotes the assembly of VP3-only VLP in E. coli	61
3.2.	Characterization of VP3 by Transmission Electron Microscopy.....	68
3.3.	Co-expression of different chaperones with VP3 promotes soluble expression and assembly of VP3 in E. coli	70
3.4.	Chaperonin increased assembled VP3 production in E. coli when co-expressed with VP3 and AAP	75
3.5.	Purification of VP3-only Virus-Like Particles.....	78
CHAPTER 4 DISCUSSION.....		85
4.1.	Summary	85
4.2.	Impact of expression conditions on expression of recombinant VP3 in E. coli .	86
4.3.	Impact of AAP on capsid assembly and protein expression of VP3 in E. coli ...	87

4.4. Impact of E. coli chaperones on capsid assembly and protein expression of VP3 in E. coli	89
4.5. Practical consideration for purification of VP3-only VLP	90
4.6. Future directions	91
REFERENCES	93

LIST OF TABLES

Table 1.1 Protein expression systems for VLP production.	4
Table 1.2 Serotypes of AAV with high transduction efficiency in major tissues.	13
Table 1.3 Essential chaperones for protein folding in <i>E. coli</i>	30
Table 2.1 Sequences of primers and oligos.	35
Table 2.2 Bacterial culture media and solutions.	38
Table 2.3 Seamless Ligation Cloning Extract (SLiCE) cloning buffers.	38
Table 2.4 Gel electrophoresis buffers.	39
Table 2.5 Western blot and dot blot buffers.	39
Table 2.6 Cell lysis and protein purification buffers.	40
Table 2.7 PCR of AAV2AAP, AAV2VP3 and T7-AAV2AAP - templates, primers and annealing temperatures.	44
Table 2.8 Thermocycling conditions for PCR of AAV2AAP, AAV2VP3 and T7- AAV2AAP.	44
Table 2.9 Plasmid vectors, antibiotics and and expression inducers used for auto- induction with LB-505	50
Table 2.10 Chromatographic conditions for protein purification.	60
Table 3.1 Expression conditions tested for expression of recombinant VP3.	63

LIST OF FIGURES

Figure 1.1 Applications of VLPs.	9
Figure 1.2 The genome of AAV.....	14
Figure 1.3 Schematic diagram of the different regions of VP1, VP2 and VP3..	14
Figure 1.4 The 3D structure of VP1 and capsid of AAV2.	17
Figure 1.5 General workflow of rAAV purification.	23
Figure 3.1 Expression vector plasmids: target protein expression of VP3 or co-expression of VP3 and AAP.	65
Figure 3.2 Expression of VP3 and co-expression of VP3 and AAP in E. coli using auto-induction method with LB-505 at 30 °C for approximately 14-16 h.....	67
Figure 3.3 Characterization of VP3 by transmission electron microscopy with negative staining.....	69
Figure 3.4 Expression vector plasmids: co-expression of VP3 with different chaperones.	72
Figure 3.5 Co-expression of VP3 with different chaperones in E. coli at 30 °C.	74
Figure 3.6 Triple co-expression of VP3 and AAP with different chaperones.....	77
Figure 3.7 Chromatography of VP3-only VLPs with Heparin column.	81
Figure 3.8 Chromatography of VP3-only VLPs with Q XL column.	82
Figure 3.9 Chromatography of VP3-only VLPs with Sephacryl S-300 HR column.	83
Figure 3.10 Chromatography of VP3-only VLPs with Heparin column (polishing)	84

LIST OF ABBREVIATIONS

AAP	Assembly-activating Protein
AAV	Adeno-associated Virus
AFM	Atomic Force Microscopy
APS	Ammonium Persulfate
ATP	Adenosine Triphosphate
CAR	Carbenicillin
CHL	Chloramphenicol
CRISPR	Clustered Regularly Interspaced Short Palindromic Repeats
DF	Diafiltration
DLS	Dynamic Light Scattering
DTT	Dithiothreitol
EDTA	Ethylenediaminetetraacetic Acid
ELISA	Enzyme-Linked Immunosorbent Assays
HIC	Hydrophobic Interaction Chromatography
HPV	Human Papillomavirus
Hsp70	Heat Shock Protein 70
HSV	Herpes Simplex Virus
IEC	Ion Exchange Chromatography
IPTG	Isopropyl β -D-1-Thiogalactopyranoside

ITR	Inverted Terminal Repeat
LB Broth	Luria Bertani Broth
MOPS	3-Morpholinopropanesulfonic Acid
NLS	Nuclear Localization Sequences
ORF	Open Reading Frames
PEG	Polyethylene Glycol
rAAV	Recombinant Adeno-Associated Virus
RBS	Ribosome Binding Sequences
RSV	Respiratory Syncytial Virus
SDS	Sodium Dodecyl Sulfate
SDS-PAGE	Sodium Dodecyl Sulfate-Polyacrylamide Gel Electrophoresis
SEC	Size Exclusion Chromatography
sHsps	Small Heat Shock Proteins
SLiCE	Seamless Ligation Cloning Extract
SPR	Surface Plasmon Resonance
TEM	Transmission Electron Microscopy
TFF	Tangential Flow Filtration
UF	Ultrafiltration
VG	Viral Genomes
VLP	Virus-Like Particle
VNP	Viral Nanoparticle

CHAPTER 1 INTRODUCTION

1.1. Virus-like particles (VLPs)

Viruses are infectious agents that require a host cell for replication¹. Normally, they are composed of viral protein coats, termed capsids, and nucleic acids. Some viruses also have envelopes. In the areas of nanobiotechnology, virus-derived agents, or viral nanoparticles (VNPs), have been developed as a new kind of nanomaterial². VLPs are a subset of VNPs that refer to those empty capsids from viruses which do not contain nucleic acids (viral genetic material). As viral capsids have many features, such as defined structure, superior stability and biocompatibility, self-assembly, and low toxicity, they have been used in different areas, such as drug delivery and imaging³.

1.1.1. Expression and purification of VLPs

1.1.1.1. Expression of VLPs

The manufacture of VLP products is usually comprised of three steps: expression, purification, and formulation. The expression of VLPs is similar to the expression of recombinant proteins and viruses⁴. First, the DNA sequences of VLP proteins are typically cloned and inserted into vectors for protein expression. Different protein expression systems have been used for VLP protein expression. Eukaryotic protein expression systems are commonly used, including baculovirus-insect cells, mammalian cells, plants, and yeast⁵.

The major advantage of these systems is that native-like capsids can usually form after expression. However, the cost and relative increased complexity are general limitations of those systems. Prokaryotic protein expression systems, like *E. coli*, have also been used. *E. coli* is a preferred expression system since it is more cost-effective than eukaryotic protein expression systems and generally provides greater versatility due to the greater simplicity of the biological system⁶. Advantages of using *E. coli* protein expression system include high expression levels, easy scale-up and short turnaround time^{7,8}. However, *E. coli* also has many limitations when used for recombinant protein expression. These limitations include: (1) inability to produce correct disulfide bonds, (2) lack of post-translational modification mechanisms present in human cells, (3) incorrect protein folding and protein aggregation, and (4) the presence of endotoxins⁹. Table 1.1 summarizes the major advantages and disadvantages of different protein expression systems.

1.1.1.2. Purification of VLPs

Purification is an essential step to ensure the appropriate efficacy and safety of VLPs, especially for clinical applications¹⁰. Before purification, pre-treatment steps are typically necessary. Depending on the expression platforms and strategies, cell lysis might be required to release the VLPs from the production cells. In some instances, such as for influenza VLPs produced in insect cells, expressed VLPs will be secreted into the culture media and thus the cell lysis process is not needed¹¹. The secretion of VLPs can also be achieved by adding a signal peptide that is recognized by the secretory pathway in the

expression vector^{10,12}. Typically, a clarification step is performed before purification to remove large contaminants, like cell debris and aggregates⁴. Many methods have been used for clarification including cell sedimentation, depth filtration and tangential flow filtration (TFF).

In the first step of VLP purification, capturing or concentration is usually applied to reduce the volume of crude samples and increase the concentration of VLPs in the samples⁴. Ultrafiltration (UF) / diafiltration (DF) and TFF are often conducted for VLP concentration, while affinity chromatography, ion exchange chromatography (IEC), and hydrophobic interaction chromatography (HIC) are performed for capturing VLPs¹³⁻¹⁵. For intermediate purification of VLPs, IEC, HIC and ultracentrifugation have been used to not only remove the contaminated proteins but also reduce concentrations of non-protein contaminants, like DNA and endotoxins. Sometimes a final purification step, or polishing step, is required to remove residual contaminants that are generated during VLP purification. IEC, size exclusion chromatography (SEC) and UF/DF are often used in polishing steps^{10,15}.

Table 1.1 Protein expression systems for VLP production.

Expression systems	Advantages	Disadvantages
Bacteria	<ul style="list-style-type: none">• Cost-effective.• Scalable.• Rapid growth.• Easy manipulation.• High-level expression.• Genetic stability.	<ul style="list-style-type: none">• Poor immunogenicity.• Recombinant proteins lack post-translational modifications.• Protein solubility issues.• Contamination by bacterial endotoxins.• Inability to create disulfide bonds.
Yeast	<ul style="list-style-type: none">• Low production cost.• No endotoxin contamination.• High-density fermentation.• Support most protein folding.	<ul style="list-style-type: none">• Lower VLP yield than <i>E. coli</i>.• High mannose modification.• Lack mammalian like post-translational modifications.
Insect cells	<ul style="list-style-type: none">• Carry and deliver large amounts of DNA.• High protein expression.• Support eukaryotic protein post-translational modifications.• Proper protein folding and assembly.	<ul style="list-style-type: none">• Difficult to scale up.• High production cost.• Baculovirus contamination.• Simpler N-glycosylation than mammalian cells.• Incomplete modification of proteins.
Mammalian cells	<ul style="list-style-type: none">• Perform proper folding, assembly, and post-translational modifications of proteins.	<ul style="list-style-type: none">• Require large-scale production facilities.• Lengthy expression time.• Low yield.• Contamination by mammalian pathogens.
Plant cells	<ul style="list-style-type: none">• High scalable.• Cost-effective.• Carry out N-glycosylation.• High expression.• Correct folding and assembly.	<ul style="list-style-type: none">• Lower VLP yield than mammalian cells.• Technical and regulatory issues.

Adapted from a published paper⁵.

1.1.2. Characterization of VLPs

Many assays and methods, both *in vitro* and *in vivo*, have been used for VLP characterization⁶. Biochemical characterization of VLPs is based on characterizations of amino acid sequences, molecular weight, conformations, and the structure of the proteins. Sodium dodecyl sulfate-polyacrylamide gel electrophoresis (SDS-PAGE) is one of the most used techniques in protein sciences. It can examine the purity, integrity and monomeric molecular weight of the VLP component proteins^{16,17}. Mass spectrometry is a more advanced and indispensable technique to determine the mass and amino acid sequences of proteins¹⁷⁻¹⁹. For measurement of secondary and tertiary structures of the VLPs, circular dichroism and ultraviolet spectroscopy have been typically used¹⁸. The stability and aggregation states of VLPs are related to the conformations and structures of the VLPs. Differential scanning calorimetry and cloud point analysis have been applied to measure the thermal stability and aggregation propensity of VLPs^{18,20-22}.

Morphological observations and actual size measurements are also important in VLP characterizations. Those characterization techniques include transmission electron microscopy (TEM)^{23,24}, dynamic light scattering (DLS), static light scattering^{25,26}, atomic force microscopy (AFM)²⁶, and analytical ultracentrifugation or density gradient ultracentrifugation²⁷. TEM can be used to determine the three-dimensional structure of VLPs. It can also provide other information like the size and number of VLPs, and VLP's

association with vesicles. However, VLP deformation might happen during TEM sample preparation. DLS is a convenient and easy technique for the measurement of the hydrodynamic size of particles, but pure VLPs are required for accurate and reliable results. AFM can also be used to measure the particle size and size distribution in ambient conditions. It can image single particles. Sample preparation of AFM is cost-effective and is less likely to cause structural deformation²⁶. Analytical ultracentrifugation or density gradient ultracentrifugation can determine the sedimentation velocity of particles, thus determining the size of VLPs²⁷.

Antibody-based methods detect functional epitopes on VLPs²⁸⁻³⁰. Those methods assess not only the binding activities of VLPs to certain antibodies *in vitro* but also the immunogenicity of VLPs *in vivo*. Various immunoassays have been used in the characterization of VLPs, including in Surface Plasmon Resonance (SPR) technology^{18,31,32}, enzyme-linked immunosorbent assays (ELISA)^{19,33,34}, dot blot assays³⁴, and immune precipitations or immune diffusion assays^{33,35}.

1.1.3. Application of VLPs

VLPs have been applied as human vaccines against infectious diseases in the past. More recently, VLP technologies have been used widely in different areas, such as drug delivery, imaging, materials, biocatalysis, and energy applications (Figure 1.1)³. However, the most common applications of VLPs are for vaccines and cargo delivery.

VLP vaccines share the structural similarity with viruses and stimulate immunity strongly in hosts. The first FDA-approved VLP-based vaccines, Recombivax HB[®], were HBsAg vaccines produced in yeast³⁶. Gardasil[®] was the second VLP-based vaccine approved by the FDA in 2006. It is used against human papillomavirus (HPV)³⁷. For now, there are only several VLP vaccines on the market³. Many VLP-based vaccines targeting different viruses like Norwalk Virus, HIV, Ebola Virus, SARS-CoV-2 Virus, Respiratory Syncytial Virus (RSV), and Influenza are still under different clinical trial stages⁴. Future directions for the development VLP vaccines include developing vaccines with broad cross-protection against different virus serotypes and vaccines with more delivery routes³. Moreover, efforts have been put into improving the thermostability of VLP vaccines since the insufficient thermostability of vaccines has restricted global vaccination delivery.

VLPs can also be used for cargo delivery in cells. VLPs have many advantages serving as drug delivery systems including: (1) self-assembly, (2) high efficiency, (3) high cargo/carrier ratio, (4) flexible modification of capsids, (5) wide variety in sizes and shapes, (6) low toxicity and great biocompatibility^{38,39}. Many therapeutic cargos can be delivered with VLPs, like chemotherapeutic drugs, protein/peptide, DNA and siRNA^{40,41}. In addition, chemical conjugation can be performed on VLPs by covalently conjugating imaging agents, such as fluorescent dyes or probes. Those modifications enable the usage of VLP in positron emission tomography and magnetic resonance imaging⁴². VLP-based single-

enzyme nanoreactors use VLPs to encapsulate active enzymes, controlling the access of reactants and products, and contributing to more stable catalytic reactions⁴³⁻⁴⁵. Moreover, VLPs can be used as robust protein cages in addition to active enzymes. For example, VLPs can be used as a delivery system with CRISPR/Cas9 in gene editing⁴⁶.

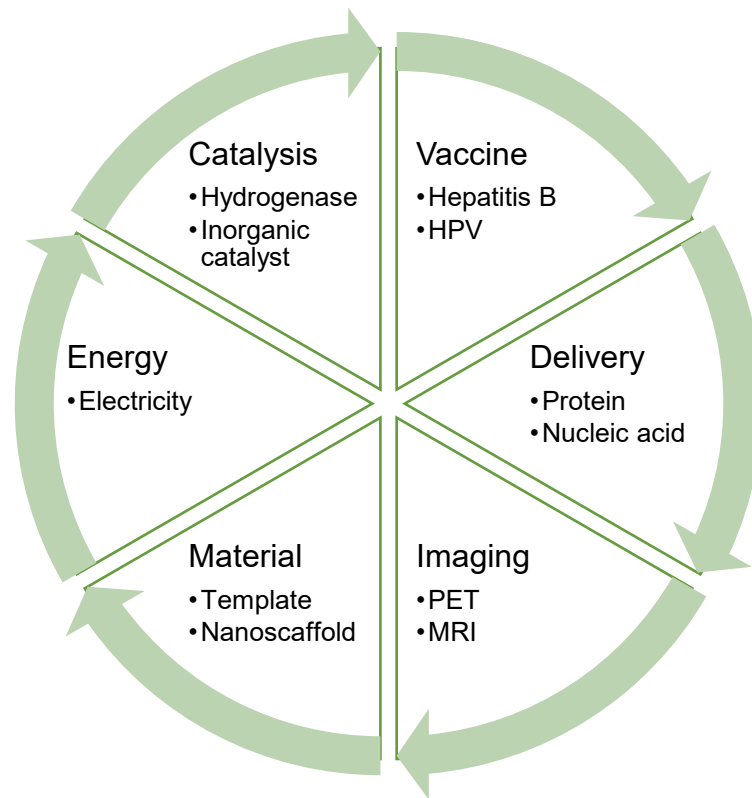


Figure 1.1 Applications of VLPs. Adapted from a published paper³.

1.2. Adeno-associated virus (AAV)

AAV is classified under the *Dependoparvovirus* genus within the *Parvoviridae* family⁴⁷. As its name suggests, the replication of AAV requires the help of a helper virus, such as adenovirus or herpesvirus⁴⁸. AAV was first discovered during preparation of adenovirus in the mid-1960s^{49,50}. Later, AAV was also been found in human tissues⁵¹. It has an icosahedral protein capsid with a diameter of around 25 nm and a single-stranded DNA genome of approximately 4.7 kb⁵². Evidence has suggested that AAV does not cause any human diseases⁵³. Many serotypes of AAV have been identified. The serotypes of AAV have different tropisms and have different transduction efficiencies in major tissues of human beings (Table 1.2)⁵⁴.

1.2.1. Genome of AAV

The genome of AAV contains two genes, *rep* and *cap*, and two inverted terminal repeats (ITRs) which flank the genes at the two ends of the genome (Figure 1.2)⁵⁵. The length of the ITR is 145 nucleotides. The initial 125 nucleotides of the ITR form a self-folding palindrome, maximizing base pairing and creating a T-shaped hairpin structure⁵⁶. The rest of the ITR is called the D sequence, which remains unpaired. ITRs hold significant importance as *cis*-acting sequences in the biology of AAVs. According to the current AAV replication model, the ITR functions as the replication origin and acts as a primer for DNA polymerase during the synthesis of the second strand. The resulting double-stranded DNA,

known as the replicating-form monomer, is then used for a subsequent round of self-priming replication, forming a replicating-form dimer. These double-stranded DNA intermediates, the replicating-form monomer and replicating-form dimer, undergo processing via a strand displacement mechanism. This yields a single strand of DNA used for packaging and a double strand of DNA used for transcription. The gene *rep* encodes four proteins, namely Rep78, Rep68, Rep52, and Rep40⁵⁶. Rep78 and Rep68 are expressed from transcripts using the P5 promoter, while Rep52 and Rep40 are produced from transcripts using the P19 promoter. Those proteins are responsible for the viral replication cycle, and exert functions involved in replication and genome package⁵⁷. The gene *cap* contributes to the assembly of the capsid⁵⁶. It was believed early on that *cap* produced three subunit proteins of the capsid using the P40 promoter: VP1, VP2 and VP3, which share the same C-terminal regions (Figure 1.3). VP1 is produced from the unspliced transcript of entire *cap* open reading frame (ORF) and the protein has a molecular weight of 87 kDa. Compared to VP2 and VP3, VP1 has a unique sequence at its N-terminus termed as VP1u. VP1u contains a phospholipase A2 (PLA2) site that plays a role in endo/lysosomal escape during cellular trafficking and viral infectivity⁵⁸. VP2 and VP3 are produced by alternative splicing with protein molecular weights of 72 kDa and 62 kDa, respectively. The sequence of approximately the first 65 amino acids at N-terminal of VP2 are termed as VP1/2 common region, which contains nuclear localization sequences (NLSs)⁵⁹. A study published in 2010, however, demonstrated that another protein, assembly-activating

protein (AAP), was also encoded by *cap*, functioning in the process of assembly of the capsid of AAV2⁶⁰.

The AAV genome integration sometimes happens at the locus known as *AAVSI* in human chromosome 19^{61,62}. Two reasons lead to the integration: (1) the sequence similarity between *AAVSI* and the ITRs, and (2) the activity of Rep proteins⁴⁷. However, random genome integration may also occur with a negligible frequency⁶³.

Table 1.2 Serotypes of AAV with high transduction efficiency in major tissues.

Tissue	Optimal serotypes
Liver	AAV8, AAV9
Skeletal muscle	AAV1, AAV7, AAV6, AAV8, AAV9
CNS	AAV5, AAV1, AAV4
Eyes	
• Retinal pigment epithelium	AAV5, AAV4
• Photoreceptor cells	AAV5
Lung	AAV9
Heart	AAV8
Pancreas	AAV8
Kidney	AAV2

Adapted from a published paper⁵⁴.

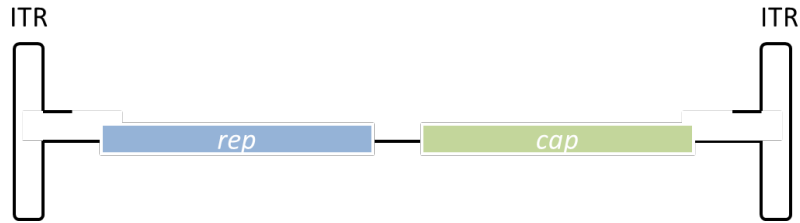


Figure 1.2 The genome of AAV. The genome is a single strand of DNA with a size of approximately 4.7 kb. The genes (*rep* and *cap*) and ITRs are indicated.

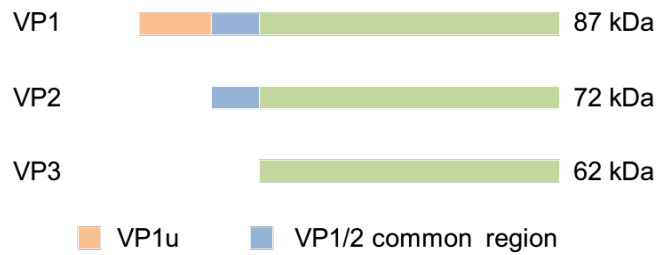


Figure 1.3 Schematic diagram of the different regions of VP1, VP2 and VP3. VP1, VP2 and VP3 share the same sequences at their C-terminal (green regions). VP1 and VP2 have VP1/2 common regions (blue regions), while VP1 has a VP1u region (yellow region).

1.2.2. Capsids of AAV

1.2.2.1. Capsid structures of AAV

The capsid of AAV is comprised of 60 subunits. Those subunits are VP1 or VP2 or VP3, and it is estimated that the ratio of VP1:VP2:VP3 in a native capsid is 1:1:10^{64,65}. However, the exact ratio of VP1, VP2 and VP3 in a capsid is determined by the relative protein levels of VP1, VP2 and VP3 expressed in the host cells. Also, each capsid may have different compositions compared to other capsids produced from the same batch⁶⁶. X-ray crystallography and cryo-electron microscopy, along with image reconstruction techniques, have been used to propose 3D models for the structures of various AAV serotypes and clonal isolates⁶⁷⁻⁷². A representative 3D model of AAV2 is shown in Figure 1.4. Notably, in the crystal structures of AAVs, the N-terminus of the AAV VP monomer, including VP1u, the VP1/2 common region, and approximately first 15 N-terminal residues of VP3, cannot be observed. Protein sequence analysis of those regions suggests that this phenomenon is caused by the existence of potential disordered regions at N-terminal of VP1 or the high flexibility of the VP1/2 common region due to glycine-rich sequences^{73,74}. However, cryo-reconstruction suggests that those regions are likely located inside the capsid⁷⁵. The remaining parts of VP proteins exhibited a structural arrangement characterized by a conserved alpha-helical region (α A) and a β A strand, followed by an eight-stranded β barrel motif⁵⁵.

1.2.2.2. Capsid assembly of AAV

The capsid assembly and genome package of AAV follow a two-step mechanism. First, the VP proteins rapidly assemble and form empty capsids. This is followed by the slower rate-limiting step of packaging the single-stranded DNA genome into the empty capsids⁷⁶. In other words, capsid assembly and genome package are two independent processes for AAV. Subsequent immunofluorescence and immunoprecipitation experiments have indicated that the VP proteins are synthesized in the cytoplasm and subsequently transported to the nucleus, particularly to the nucleoli where capsid assembly takes place⁷⁷. This transportation is facilitated by nuclear localization signals found on the N-terminus of the VP, within VP1u and VP1/2 common regions. Moreover, sedimentation sucrose gradient analysis of nuclear and cytoplasmic fractions during an AAV infection have revealed significant findings. The cytoplasmic fraction was found to contain a population of VP monomers and oligomers, ranging in size from 10 to 15S, which aligned with the sedimentation coefficients typical for trimers and pentamers of VP1, VP2, and VP3. In contrast, the nuclear fraction contained VP oligomers with sedimentation coefficients ranging from 60 to 110S, indicating the presence of both empty and fully packaged capsids⁷⁸.

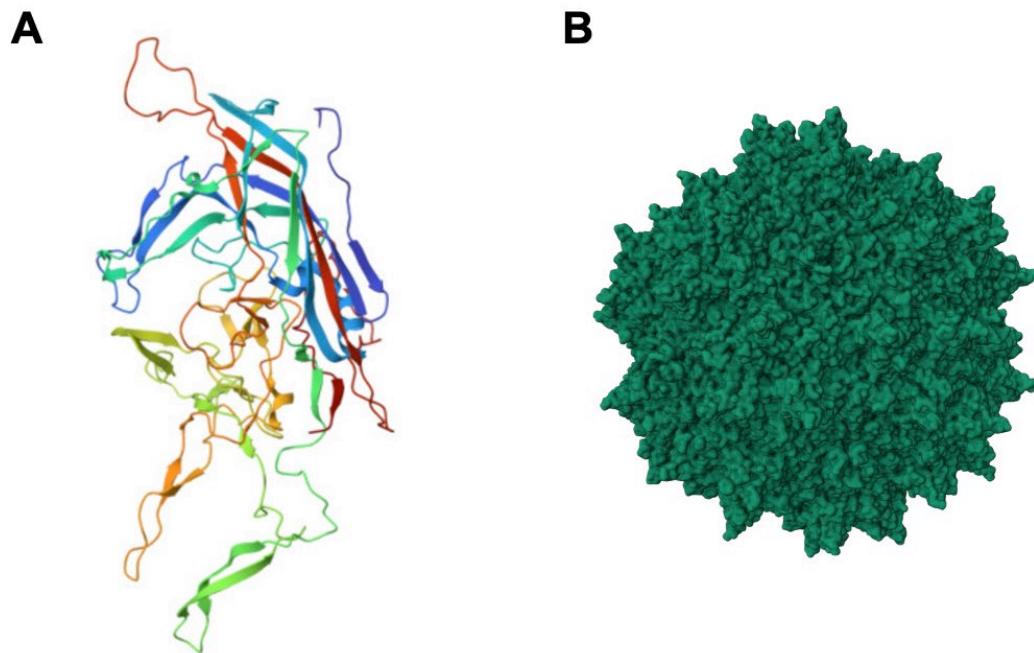


Figure 1.4 The 3D structure of VP1 and capsid of AAV2. (A) Ribbon diagram of VP3 protein model determined by cryo-electron microscopy⁷⁹. (B) The 3D structure of assembled capsid⁷⁹. The images were generated from PDB Database using PDB# 6IH9⁷⁹.

The exact mechanism for AAV capsid assembly is still unclear. Mutations on *cap* gene have shown that VP3-only capsids can still be produced in host cells when the start codons of VP1 and VP2 were mutated into other sequences⁸⁰⁻⁸³. However, VP3 cannot self-assemble in host cells when expressing VP3 alone with truncated *cap* gene⁸¹. It was found later that AAP was also essential for AAV capsid assembly in host cells⁶⁰. Studies on AAP's functions suggest that AAP may serve as a chaperone or scaffold protein during capsid assembly⁸⁴. Yet it is not clear whether AAP is indispensable for all serotypes of AAVs, since some studies have shown that several AAVs, such AAV4, AAV5 and AAV11, do not need AAP for capsid assembly⁸⁵.

1.2.3. Production of recombinant AAV (rAAV) and AAV-based VLPs

Many protein systems have been developed for production of rAAVs. Initially, HeLa-based stable cell lines infected with adenovirus were used for rAAV production⁴⁷. In this method, HeLa cells are stably transfected with *rep* and *cap* genes and the sequences of interest flanked by ITR sequences⁸⁶. Adenovirus is then transduced into the cells to begin the induction of expression of rAAV. However, there are two primary drawbacks to this approach which impeded the widespread adoption of this technology. First, developing a new cell line is necessary for each combination of capsid and the gene of interest to be delivered⁴⁷. Second, the introduction of adenovirus complicates the process.

Nowadays, transient plasmid DNA transfection in mammalian cells to produce rAAV is the most widely used method for rAAV production⁴⁷. Generally, three plasmids are used for transfection: one for expression of the adenoviral proteins that AAV needs, one for expression *cap* and *rep* gene of AAV and one for expression of sequences of interest flanked by ITR sequences⁸⁷. The two-plasmid transfection system is also used for rAAV production. In this system, the *rep* and *cap* genes of AAV and helper genes of adenovirus are on the same plasmid⁸⁸. For transfection, the HEK-293 cell line is generally used⁸⁹. To scale up the expression and increase rAAV yields, suspension cell culture has been developed based on adapted HEK-293 cells⁹⁰. The advantages of this system include: (1) new construction of AAVs can be produced and tested in a short time⁸⁷; (2) there are no adenovirus contaminants after expression. However, a notable disadvantage related to this system involves the potential inclusion of plasmid backbone sequences in the rAAV, which may trigger the activation of the innate immune system and the expression of antibiotic resistance genes on the plasmid backbone^{91,92}.

An alternative approach to produce rAAV involves infecting mammalian cells, such as HEK-293 or BHK cells, with replication-deficient herpes simplex virus (HSV)^{93,94}. Typically, this method employs two HSV vectors: one for expressing the gene of interest that is flanked by the two ITR sequences, while the other for expressing *rep* and *cap* of rAAV^{87,94}. This strategy has shown promise in generating rAAV stocks with enhanced viral

potency^{94,95}. However, rAAV produced using this system may contain contaminating HSV and its products⁸⁷.

In addition to human cells, rAAV can be produced in insect cells, like Sf9, with recombinant baculovirus infection⁹⁶. The primary advantage of the baculovirus-insect cell system is that high titer rAAV can be achieved at one time with a yield exceeding 10^{16} viral genomes (VG) produced from bioreactors of 200 L⁹⁷. In addition, Sf9 cells do not require additional helper viral genes since recombinant baculovirus can replace them to support rAAV production⁹⁸. Moreover, baculovirus-insect systems also demonstrate reduced encapsidation of contaminating DNAs⁴⁷. However, it's important to note that baculovirus-insect and human manufacturing platforms can produce rAAV with chemical and functional differences, like variations in capsid post-translational modifications, insect and baculoviral impurities and potentially lower packaging percentages compared to human cell-produced rAAVs⁹⁹.

AAV-based VLPs were successfully produced in the protein expression systems mentioned above^{80,100}. In addition to eukaryotic expression systems, researchers have studied its production in *E. coli*. For example, Le et al. (2022), have successfully produced VP3-only capsids of AAV5, an AAP-independent serotype of AAV, in *E. coli*¹⁰¹. Moreover, VLPs can be produced *in vitro* by protein refolding and/or *in vitro* capsid assembly^{102,103}. For example, Le et. al. (2019), found that AAV2 VP3 formed inclusion bodies when expressed

in *E. coli*, and AAV2 VLPs can be produced *in vitro* after renaturation and capsid assembly¹⁰².

1.2.4. Purification of rAAV

Purification of rAAV is necessary to removal harmful substances and enhance the transduction efficiency. The cells after rAAV expression cannot be used for purification directly, some pre-treatment must be conducted before purification. Those pre-treatments are similar to pre-treatments used for VLP purification (see 1.1.1.2). For purification, many methods have been applied, including density gradient ultracentrifugation and chromatographic methods. A general workflow of purification of rAAV is shown in Figure 1.5.

1.2.4.1. Density gradient ultracentrifugation

For over six decades, ultracentrifugation has served as a widely employed technique for purifying viral preparations in laboratory settings¹⁰⁴. This method involves the use of "density gradient media", like solutions of cesium chloride (CsCl), sucrose, and iodixanol (OptiPrep), to establish gradients¹⁰⁵. The separation of the virus from other components in the samples is based on their sedimentation characteristics, which are defined by factors such as molecular weight, shape, partial specific volume, and the reciprocal particle density value. The density of rAAV ranges from 1.40 to 1.42 g/cm³, distinguishing it from contaminants like genomic DNA (density of 1.7 g/cm³) and RNA (density of 2.0 g/cm³).

Nevertheless, some cellular components, such as proteins (with densities between 1.2 and 1.4 g/cm³), chromatin (density of 1.4 g/cm³), and certain organelles (densities between 1.1 and 1.6 g/cm³) in transfected cells closely resemble the density of rAAV, and thus ultracentrifugation cannot remove those contaminants. Additionally, it's important to consider the density of empty capsid (1.31 to 1.32 g/cm³) of rAAV in ultracentrifugation¹⁰⁶.

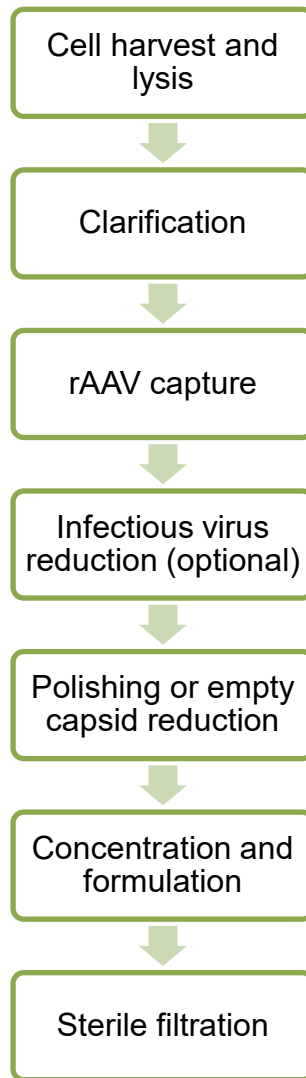


Figure 1.5 General workflow of rAAV purification. After cell harvest, cell lysis is performed followed by clarification. The clarified lysates (sometimes combined with filtered cell culture medium) were used for purification. If the infectious virus (*e.g.* adenovirus) is used for rAAV expression, a step to reduce the infectious virus needs to be conducted. After purification, rAAV concentration and formulation as well as sterile filtration are generally performed to get the final products.

Cesium chloride (CsCl) gradient ultracentrifugation is effective in separating viral vectors, and it can separate full and empty capsids. However, mass spectrometry analysis has unveiled the presence of notable protein impurities following CsCl ultracentrifugation due to the similarity in density between impurities and rAAV¹⁰⁷. In addition, this method demands a considerable amount of labor and time to perform. It necessitates two or three rounds of ultracentrifugation to achieve high purity of rAAV after purification, and each turn takes 12 to 36 hours^{107,108}.

Iodixanol gradient ultracentrifugation operates on the principle of isolating rAAV-containing components from cell lysate based on their density and size in pre-established, stepwise gradients of iodixanol solutions at 15%, 25%, 40%, and 60%¹⁰⁹. Ultracentrifugation is carried out at speeds exceeding 345,000 g for approximately 130 minutes. After ultracentrifugation, cellular proteins and debris stay at the boundary between the 25% and 40% gradients, while rAAV are concentrated between the 40% and 60% gradients with a density of 1.23 g/ml³.

1.2.4.2. Hydrophobic Interaction Chromatography

HIC relies on the interaction between hydrophobic ligands (either aliphatic or aromatic) present on the stationary phase and hydrophobic residues on the protein surfaces¹¹⁰. Hydrophobic residues of proteins are usually present internally in the final native protein conformations. Kosmotropic salts, such as ammonium sulfate, sodium citrate, and

potassium phosphate, expose the hydrophobic residues of proteins by interacting with water molecules, thereby enhancing protein-ligand interactions in HIC¹¹¹.

When purifying rAAV with HIC, rAAVs are generally found to bind to the column in a high ionic strength buffer, typically containing 1 to 2 M ammonium sulfate¹¹². Subsequently, elution is achieved by reducing the salt concentration. This method has been applied in purification of several serotypes of AAV with approximately 87% recovery of rAAV from the sample on average¹¹³. HIC offers limited resolution for rAAV purification since some other proteins are eluted under these conditions. Additionally, the high salt solution carries a risk of promoting rAAV aggregation, making it less commonly used for rAAV purification¹¹².

1.2.4.3. Ion Exchange Chromatography

IEC facilitates the separation of proteins through the electrostatic interaction between ions on the protein surfaces and ionic functional groups carrying the opposing charges bound to the solid phases¹¹⁴. IEC can be categorized into cation exchange chromatography and anion exchange chromatography based on the charges of the functional groups that the solid phases have during purification.

The isoelectric points of rAAVs and the pH of the buffers used for purification determine whether anion exchange chromatography or cation exchange chromatography should be

used¹¹². When the pH of the buffers is higher than the isoelectric point of rAAV, rAAV will generally display a negative charge on their surface. Consequently, anion exchange resins are employed. For instance, alkaline pH values are utilized for effective binding of rAAV8, while pH values below 7 are employed for binding rAAV5 with anion exchange resin¹¹⁵. Conversely, at pH levels below the isoelectric point of rAAVs, rAAV acquire a positive charge. In such instances, separation is carried out using cation exchange resins.

One of the advantages of using ion exchange chromatography is that empty capsid and rAAV (genome-containing vectors) can be separated with this method¹⁰⁵. The separation is based on the differences of isoelectric points of empty capsid and rAAV. For an empty capsid of rAAV, the average calculated value of isoelectric points is 6.3. And for rAAVs, the average calculated value of isoelectric points is 5.9⁷³. Therefore, empty capsids will be eluted first in anion exchange chromatography, while rAAVs will be eluted first in cation exchange chromatography.

1.2.4.4. Size Exclusion Chromatography

SEC is a method that primarily separates proteins based on their size and apparent molecular weight. It is also helpful in evaluating the proportions of rAAV aggregates and capsid fragments, as well as the purities of rAAVs¹¹⁶. For purifying rAAVs through SEC, resins need to have an average pore size smaller than the diameter of the rAAV capsid¹⁰⁵. This ensures that rAAV particles are not trapped in the resin and are eluted in the void

volume¹¹⁷. In contrast, macromolecular impurities are delayed by crossing the pores of the resins and eluted in later fractions. A widely used resin for this purpose is the Superdex 200 (Cytiva, MA), which possesses an exclusion limit (the maximum mass of particles that can enter the resin pores) of about 1.3×10^6 Da¹¹⁸.

Generally, SEC is used in the final polishing step if rAAV samples when high purity is needed¹¹⁴. It can efficiently remove contamination like cellular peptides, which are hard to remove with other techniques^{119,120}. For instance, SEC has been employed for the final purification of rAAV1^{118,120,121}, rAAV5¹²², rAAV8¹²³, and rAAV9¹²⁴.

1.2.4.5. Heparin Affinity Chromatography

The capsid protein's surface structure of AAV plays a pivotal role in AAV's ability to bind to the receptors in target cells for transduction¹²⁵. Heparan sulfate proteoglycan is one of the receptors that AAV2 uses for transduction¹²⁶. Consequently, heparin-based affinity chromatography has proven successful in purifying rAAV2 vectors¹²⁷. Other serotypes of rAAVs have also shown the ability to bind to heparin, but only mutation of one amino acid may compromise this ability. For example, it was shown that the heparin-binding capability of rAAV6 could be attenuated through the AAV6-K531E mutation¹²⁸. On the other hand, mutations can also enhance some rAAVs' binding to heparin. For instance, rAAV8 gained heparin binding ability through the rAAV8-E533K mutant¹²⁸.

1.2.4.6. Immunoaffinity Chromatography

Immunoaffinity chromatography is dependent on the interaction between antigen and antibody to selectively purify target proteins¹⁰⁵. Recently, several affinity resins for rAAV purification have been developed based on single-chain camelid VH (heavy chain variable region) antibodies covalently linked to the matrix¹²⁹. For example, AVB Sepharose resin (Cytiva, MA) can be used to purify rAAV1, rAAV2, rAAV5, or rAAV6¹³⁰. For purification of rAAV8 and rAAV9, POROS™ CaptureSelect™ AAV8 and AAV9 (Thermo Fisher Scientific, MA) can be used respectively. POROS™ CaptureSelect™ AAVX show affinity for many serotypes, including AAV1-9, thus being widely used for the purification of native and chimeric rAAVs¹³¹. Those resins have gained interests from the industry since purification with those resins can be easily scale-up and meet the requirements of good manufacturing practice¹²⁹.

1.3. Chaperones and protein folding in *E. coli*

Chaperones play a critical role in assisting in the correct folding of newly synthesized polypeptides into proteins with native conformation and in maintaining the quality control of the proteome by refolding misfolded or aggregated proteins¹³². Within the cytosol of *E. coli*, the following chaperone systems contribute to this essential function (Table 1.3)¹³³: (1) the ribosome-associated Trigger Factor; (2) the DnaK system (also known as Hsp70), consisting of DnaK along with its co-chaperones DnaJ and GrpE; and (3) the GroEL system

(also known as chaperonin), comprising GroEL and its co-chaperone GroES¹³⁴. Hsp70 and chaperonin not only aid in the folding of newly synthesized polypeptides, but also prevent aggregation and promote the refolding of existing proteins that have lost their native conformation due to factors such as thermal denaturation or intrinsic instability^{135,136}. Additionally, Hsp70 collaborates with ClpB to solubilize aggregated proteins and refold them to their native state, working in concert with chaperonin¹³⁷⁻¹³⁹.

When it comes to the overproduction of recombinant proteins in host cells, issues related to misfolding and aggregation commonly occur¹⁴⁰⁻¹⁴². These problems often arise due to the limited folding capacity of the host cell's chaperone machinery. Researchers have tested co-expression of specific chaperones with recombinant proteins in the host cells to enhance the yield of correctly folded and soluble recombinant proteins. However, these efforts have seen only limited success¹⁴³⁻¹⁴⁵.

Table 1.3 Essential chaperones for protein folding in *E. coli*.

Chaperone family	Proteins in <i>E. coli</i>	Co-chaperones	Functions
Trigger factor	Trigger factor	-	<ul style="list-style-type: none">▪ ATP-independent▪ Ribosome-associated chaperone▪ <i>De novo</i> protein folding
Hsp70	DnaK	DnaJ, GrpE	<ul style="list-style-type: none">▪ ATP-dependent▪ <i>De novo</i> protein folding▪ Prevention of protein aggregation at high temperature▪ Regulation of the heat shock response▪ Disaggregation of protein aggregates together with ClpB
Chaperonin	GroEL	GroES	<ul style="list-style-type: none">▪ ATP-dependent▪ <i>De novo</i> protein folding▪ Prevention of protein aggregation at high temperature

Adapted from a published paper¹³³.

1.4. Goal of the study

It has been suggested that VP3 of AAV2 can assemble and form VP3-only capsids in human cells and insect cells with the help of AAP⁸⁴. Moreover, while recombinant VP3 of AAV2 can be produced in abundance in *E. coli*¹⁰², to our knowledge, the generation of VP3-only VLPs in *E. coli* has not been demonstrated. While robust recombinant protein expression can be achieved, VP proteins are typically found in inclusion bodies. The goal of this study is to explore the possibilities for production of VP3-only VLPs in *E. coli*.

1.4.1. Hypothesis

Native-like VP3-only AAV2 VLPs may be produced in *E. coli* under co-expression with AAP and/or other *E. coli* chaperones.

1.4.2. Objective

Investigate and develop methods to produce VP3-only AAV2 VLP in *E. coli*.

1.4.3. Specific aims

1) Investigate and optimize expression conditions to obtain soluble AAV2 VP3 in *E. coli*.

- 2) Investigate the potential to produce AAV2-based VP3-only VLPs in *E. coli* under co-expression with the AAP and/or *E. coli* chaperones.
- 3) Develop purification protocols for putative AAV2-based VP3-only VLPs produced in *E. coli*.

CHAPTER 2 MATERIALS AND METHODS

2.1. Materials

2.1.1. Regents for bacterial culture and protein expression

Tryptone and yeast extract were purchased from Thermo Fisher Scientific, MA. Glucose was purchased from AMERSCO, MA. Sodium chloride was purchased from J.T.Baker, PA. Potassium dihydrogen phosphate, ammonium sulfate, sodium hydrogen phosphate heptahydrate, lactose and glycerol were purchased from VWR, PA. Isopropyl β -D-1-thiogalactopyranoside (IPTG) was purchased from Growcells, CA. Chloramphenicol was bought from Acros Organics, NJ. L-Arabinose was purchased from Thermo Scientific, MA. Carbenicillin Solution (100mg/mL) was purchased from Teknova, CA. Luria Bertani (LB) Agar, Miller was purchased from BD, NJ.

2.1.2. Molecular cloning reagents

Q5[®] Hot Start High-Fidelity DNA Polymerase, Instant Sticky-end Ligase Master Mix, T4 polynucleotide kinase and all restriction enzymes (*Xba*I, *Nde*I, *Bam*HI and *Hind*III) were purchased from New England Biolabs, MA. dNTP Mix was purchased from Promega, WI. E.Z.N.A.[®] Plasmid DNA Mini Kit I and E.Z.N.A.[®] Cycle Pure Kit were purchased from Omega Bio-Tek, GA. Dithiothreitol (DTT) and Triton-X 100 were purchased from Sigma-Aldrich, MA.

2.1.3. Plasmids and vectors

pDG vector was a gift from Dr. Ashley Martino (St. John's University). pET15b plasmid was purchased from MilliporeSigma, MA. Chaperone plasmid set (pTf16, pKJE7 and pGro7) was purchased from Takara Bio, CA.

2.1.4. Antibodies

Anti-Adeno-associated virus (AAV2), intact particles, clone A20 and Anti-Adeno-associated virus (AAV), VP1/VP2/VP3, clone B1 were purchased from American Research Products, MA. Anti-His-tag antibody was purchased from GenScript, NJ. Peroxidase-conjugated affinipure goat anti-mouse IgG (H+L) was purchased from Rockland, PA. Goat anti-rabbit IgG (H&L) HRP conjugate was purchased from Jackson Immunoresearch, PA.

2.1.5. Primers and oligos

The primers and oligos are shown in Table 2.1. All primers and oligos were purchased from Fisher Scientific, MA, using the Invitrogen custom DNA oligos synthesis service.

Table 2.1 Sequences of primers and oligos.

NdeI-AAV2VP3-F	AATCATATGGCTACAGGCAGTGGC
BamHI-AAV2VP-R	AGAGGATCCTTACAGATTACGAGTCAGGTAT C
NdeI-AAV2AAP-F	CGTCATATGGAGACGCAGACTCAG
BamHI-AAV2AAP-R	AAAGGATCCTCAGGGTGAGGTATCCAT
Homo-AAV2VP3-BamHI-T7- AAP-F	ACTCGTAATCTGTAAGGATCCTCGATCCCGC GAAATTAATACG
Homo-T7term-HindII-AAP-R	GTTTGACAGCTTATCATCGATAAGCTT
XbaI-delta-His-F	CTAGAAATAATTTTGTTTAACTTTAAGAAGG AGATATACA
NdeI-delta-His-R	TATGTATATCTCCTTCTTAAAGTTAAACAAA ATTATTT

2.1.6. Other reagents and materials

Syringe filter with 0.22 μm cellulose acetate membrane, methanol, ethanol, Tris and Tween-20 were purchased from VWR, PA. Potassium acetate, ethylenediaminetetraacetic acid (EDTA), glacial acetic acid, ammonium persulfate (APS), glycine, sodium dodecyl sulfate (SDS) and bromophenol blue were bought from J.T.Baker, PA. β -mercaptoethanol was bought from MP Biomedicals, CA. Sodium bisulfate was purchased from Fisher Scientific, MA. Triton X-114, Acrylamide/Bis solution (40%, 37.5:1), Bis-tris and urea were purchased from Thermo Scientific, MA. 3-morpholinopropanesulfonic acid (MOPS) and Commassie Blue G-250 were purchased from TCI Chemicals, OR. Milk powder was purchased from Rockland Immunochemicals, PA. Polyethylene glycol (PEG) 8000 was purchased from Alfa Aesar, MA. Potassium chloride was purchased from BDH, PA. Optiprep density gradient media (60% (w/v) iodixanol) was bought from Cosmo Bio, CA. Supersignal west pico PLUS chemiluminescent substrate, Pierce™ Silver Stain Kit and Gibco™ Pluronic™ F-68 non-ionic Surfactant (100X) were purchased from Thermo Fisher Scientific, MA. Benzoyl-DL-phenylalanine (Bz-DL-Phe) was purchased from MilliporeSigma, MA. Polyethyleneimine, approx. M.N. 60,000, 50 wt.% aq. Solution and Ponceau S were purchased from Acros Organics, NJ. 300-mesh copper grid with formvar and carbon coatings and UranylLess were bought from Electron Microscopy Sciences, PA. BioTrace NT nitrocellulose transfer membrane was purchased from Pall Corporation, NY. C 16/70

column, HiTrap Q XL, HiTrap Heparin HP and Sephacryl S-300 HR were purchased from Cytiva, MA.

2.2. Buffers and solutions

Table 2.2 Bacterial culture media and solutions.

LB broth	1% (w/v) Tryptone, 0.5% (w/v) yeast extract, 1% (w/v) NaCl
LB agar	1.5% (w/v) agar in LB broth with appropriate antibiotics (100 µg/ml carbenicillin or/and 25 µg/mL chloramphenicol)
50X 505	25% (w/v) glycerol, 2.5% (w/v) glucose.
20X P	0.5M (NH ₄) ₂ SO ₄ , 1M KH ₂ PO ₄ , 1M Na ₂ HPO ₄ ·7H ₂ O
ZYP-5052	1% (w/v) Tryptone, 0.5% (w/v) yeast extract, 0.2% (w/v) lactose, 1mM MgSO ₄ , 1X 505, 1X P
LB-505	1X 505 in LB broth

Table 2.3 Seamless Ligation Cloning Extract (SLiCE) cloning buffers.

SLiCE extract lysis buffer	50 mM Tris pH 8.0, 3% (w/v) Triton X-100
10X SLiCE buffer	500mM Tris pH7.5, 100mM MgCl ₂ , 10mM ATP, 10mM DTT

Table 2.4 Gel electrophoresis buffers.

5X SDS loading buffer	312.5 mM Tris, 10% (w/v) SDS, 50% (v/v) glycerol, 0.025% (w/v) Bromophenol blue, 25% (v/v) β -mercaptoethanol
200X sodium bisulfite	1 M sodium bisulfite
5X MOPS-SDS running buffer	250 mM MOPS, 250 mM Tris, 5 mM EDTA, 0.5% (w/v) SDS
3X Bis-tris gel buffer (pH 6.5-6.8)	1 M Bis-Tris
50X TAE	2 M Tris, 1 M glacial acetic acid, 50 mM EDTA
10% bis-tris separating gel (10 mL)	4.2 mL of water, 3.3 mL of 3X gel buffer, 2.5 mL of 40% acrylamide, 100 μ L of 10% APS, 10 μ L of TEMED
5% bis-tris stacking gel (5 mL)	2.7 mL of water, 1.6 mL of 3X gel buffer, 0.625 ml of 40% acrylamide, 50 μ L 10% APS, 10 μ L of TEMED

Table 2.5 Western blot and dot blot buffers.

10X TBS (pH 7.5)	1.5 M NaCl, 200 mM Tris
1X TBST	0.1% (v/v) Tween-20 in 1X TBS
10X Tris-glycine buffer	250 mM Tris, 1.92 M of glycine
1X Tris-glycine wet transfer buffer	20% (v/v) methanol in 1X Tris-glycine buffer
Ponceau S staining solution	0.5% (w/v) Ponceau S, 1% (v/v) acetic acid
Blocking solution	5%(w/v) nonfat milk powder in TBST

Table 2.6 Cell lysis and protein purification buffers.

10X PBS (pH 7.4)	1.4 M NaCl, 25 mM KCl, 150 mM Na ₂ HPO ₄ ·7H ₂ O, 16.2 mM KH ₂ PO ₄
PBS (pH 7.4)	1X PBS in distilled water
PBS-MK (high salt)	Add 1 M NaCl, 2.5 mM KCl, and 1 mM MgCl ₂ in 1X PBS
PBS-MK (low salt)	Add 100 mM NaCl, 2.5 mM KCl, and 1 mM MgCl ₂ in 1X PBS
PEG stock solution	40% (w/v) PEG 8000, 2.5 M NaCl
PEI stock solution (pH 7.9)	10 % (v/v) PEI
Purification Buffer A	20 mM Tris pH 8.5, 5 mM MgCl ₂ , 0.001% (v/v) Pluronic F-68
Purification Buffer B	20 mM Tris pH 8.5, 5 mM MgCl ₂ , 1 M NaCl, 0.001% (v/v) Pluronic F-68
Purification Buffer C	Add 0.001% (v/v) Pluronic F-68 in PBS
Purification Buffer D	Add 1 M NaCl, 0.001% (v/v) Pluronic F-68 in PBS
Purification Buffer E	20 mM Tris pH 8.5, 5 mM MgCl ₂ , 300 mM NaCl, 2.5 M Urea, 0.001% (v/v) Pluronic F-68

2.3. Methods

2.3.1. Plasmid construction

2.3.1.1. DNA mini-prep plasmid preparation and DNA sequencing

All DNA mini-prep plasmid preparation was performed using the E.Z.N.A.® Plasmid DNA Mini Kit I as per the manufacturer's instruction. The sequences of all plasmid constructs were verified by Sanger DNA sequencing. All DNA sequencing was performed by Genewiz, NJ.

2.3.1.2. Construction of pET15b-ΔHis

The pET15b-ΔHis expression vector was constructed from the commercially available pET15b vector by deleting the His-tag coding sequence using the annealed oligo cloning method¹⁴⁶. The pET15b vector was digested with *Xba*I and *Nde*I then purified with the E.Z.N.A.® Cycle Pure Kit. *Xba*I-delta-His-F and *Nde*I-delta-His-R oligos (see Table 2.1 for sequences) were phosphorylated with T4 polynucleotide kinase in a reaction that contained 10 μM of oligos, 5 U T4 polynucleotide kinase, 1 mM ATP and 1X T4 Polynucleotide Kinase Reaction Buffer, which was incubated at 37 °C for 30 min as per the manufacturer's instruction. Oligos were annealed by incubation at 95 °C for 5 min and then the temperature was lowered at a rate of 5 °C/min in a Mastercycler Personal PCR thermocycler (Eppendorf, NY). The annealed oligos (approximately 10 μM) were diluted

200 times to approximately 0.05 μM with nuclease-free water. Then ligation was performed in a 10 μL volume containing 50 μg of purified digested plasmid, 1 μL of diluted annealed oligos, 5 μL of 2X Instant Sticky-end Ligase Master Mix. Ligation mixtures were transformed into *E. coli* (DH5 α) by heat shock method for mini-prep plasmid preparation and DNA sequencing.

2.3.1.3. PCR amplification of AAV2VP3, AAV2AAP and T7-AAV2AAP

All PCR assays were performed using Q5 Hot Start High-Fidelity DNA Polymerase in the Mastercycler Personal PCR thermocycler. Reactions contained 1X Q5 Reaction Buffer, 200 μM of dNTPs, 0.5 μM of forward primer and reverse primer, 1 ng of template DNA, 0.02 U/ μL of Q5 Hot Start High-Fidelity DNA Polymerase and nuclease-free water. The reaction conditions are given in Tables 2.7 and 2.8. All PCR products were purified with E.Z.N.A.® Cycle Pure Kit.

2.3.1.4. Construction of pET15b- Δ His-VP3 and pET15b-AAP

For construction of pET15b- Δ His-VP3 and pET15b-AAP, PCR products of insert DNA, pET15b- Δ His and pET15b were digested with *NdeI* and *BamHI* and purified with the E.Z.N.A.® Cycle Pure Kit. Ligation reactions were then performed to insert AAV2VP3 into pET15b- Δ His and insert AAV2AAP into pET15b using Instant Sticky-end Ligase Master Mix as per manufacturer's instruction. The molar ratio of inserts to digested

plasmids in the reactions was 3:1. Ligation mixtures were transformed into *E. coli* (DH5 α) by heat shock method for mini-prep plasmid preparation and DNA sequencing.

Table 2.7 PCR of AAV2AAP, AAV2VP3 and T7-AAV2AAP - templates, primers and annealing temperatures.

Product	Template	Primers	Annealing temperatures
AAV2VP3	pDG	NdeI-AAV2VP3-F, BamHI-AAV2VP3-R	61 °C
AAV2AAP	pDG	NdeI-AAV2AAP-F, BamHI-AAV2AAP-R	61 °C
T7-AAV2AAP	pET15b-AAV2AAP	Homo-AAV2VP3-BamHI-T7-AAV2AAP-F, Homo-T7term-HindII-AAV2AAP-R	65 °C

Table 2.8 Thermocycling conditions for PCR of AAV2AAP, AAV2VP3 and T7-AAV2AAP.

Step	Condition	Temperature	Time
1	Initial Denaturation	98 °C	1 min 30 s
2	Denaturation	98 °C	10 s
3	Annealing	61 °C or 65 °C (see details in Table 2.7)	30 s
4	Extension	72 °C	2 min
5	Repeat step 2-4 for 30 cycles		
6	Final Extension	72 °C	2 min
7	Storage	4 °C	∞

2.3.1.5. SLiCE extract preparation

The preparation of SLiCE extract was based on the published protocol¹⁴⁷. A single colony of *E. coli* (JM109) was inoculated into 3 mL of LB broth and incubated overnight (approximate 14-16 h) at 37 °C with shaking at 250 rpm in the MAXQ 4000 shaking incubator (Thermo Scientific, IL). The next day, 1 mL of overnight culture was transferred into 50 mL of LB broth and incubated with shaking until O.D._{600nm} reached approximately 2 to 3. Cells were collected by centrifuging at 4,600 x g for 10 min at 4 °C in a TX-400 Swinging Bucket Rotor fitted into a Heraeus™ Multifuge™ X1R centrifuge (Thermoscientific, Rockford, IL). The supernatant was discarded, and the pellet was suspended with 25 mL of distilled water and followed by centrifugation at 4,600 x g for 10 min at 4 °C. Supernatant was discarded and the pellet was resuspended in 1.2 mL of SLiCE extract lysis buffer. After 10 min of incubation on ice, the lysate was centrifuged at 20,000 x g for 2 min in a Sorvall Legend Micro 21 centrifuge (Thermo Scientific, IL). The supernatant was transferred to a 1.5 mL tube and an equal amount of ice-cold 80% glycerol was added to the tube, then mixed gently and aliquoted in 50 µL. Aliquots were frozen by incubation in liquid nitrogen then stored at -80 °C.

2.3.1.6. Construction of pET15b-ΔHis-VP3-AAP

pET15b-ΔHis-VP3-AAP was constructed by SLiCE cloning^{147,148}. The vector pET15b-ΔHis-VP3 was linearized by digestion with *Bam*HI and *Hind*III and purified using the

E.Z.N.A.® Cycle Pure Kit. A 10 µL SLiCE reaction was performed by mixing insert fragment (T7-AAV2AAP), linearized plasmid, 1 uL of 10X SLiCE buffer, 1 µL SLiCE extract and water. The molar ratio of insert to linearized plasmid in the reaction was 3:1. The mixture was incubated at 37 °C for 15 min, then transformed into *E. coli* (DH5α) by heat shock method for mini-prep plasmid preparation and DNA sequencing.

2.3.2. Recombinant protein expression in *E. coli*

2.3.2.1. Traditional IPTG-based induction of recombinant VP3 expression

Protein expression was performed based on standard pET vector expression protocols as provided from the manufacturer. A colony of *E. coli* (BL21(DE3)) transformed with pET15b-ΔHis-VP3 from freshly streaked plates was picked to inoculate 3 mL of LB broth containing 1% (w/v) glucose and 100 µg/mL of carbenicillin. The culture was incubated at 37°C overnight (approximately 14-16 h) with shaking at 250 rpm in the MAXQ 4000 shaking incubator. The next day, 60 µL of starter culture was used to inoculate 3 mL of LB broth containing 100 µg/mL of carbenicillin in a 14 mL test tube. The inoculated bacterial culture was incubated at 37°C with shaking at 250 rpm in the MAXQ 4000 shaking incubator until O.D._{600nm} reached approximately 0.6-1.0. IPTG (0.1 mM or 1 mM) was added to the bacterial culture and the culture was incubated at different temperatures (16°C, 25°C, 30 °C or 37 °C as indicated) for the indicated time (see 3.1 for details). 1 mL of bacterial culture was taken for centrifugation at 21,000 x g for 1 min with a Sorvall Legend

Micro 21 centrifuge. The supernatant was discarded and the cell pellet was used for SDS-PAGE (see 2.3.4). Another 1 mL of bacterial culture was taken for cell lysis (see 2.3.3.1).

2.3.2.2. Auto-induction of recombinant VP3 using ZYP-5052

Auto-induction with ZYP-5052 was performed based on published protocol¹⁴⁹. A colony of *E. coli* (BL21(DE3)) transformed with pET15b-ΔHis-VP3-AAP from freshly streaked plates was picked to inoculate 3 mL of LB broth containing 1% (w/v) glucose and 100 µg/mL of carbenicillin. The culture was incubated at 37°C overnight (approximately 14-16 h) with shaking at 250 rpm in the MAXQ 4000 shaking incubator. 60 µL of starter culture was used to inoculate 3 mL of ZYP-5052 containing 0.025 mM IPTG and 100 µg/mL of carbenicillin in a 14 mL test tube. Cultures were incubated at different temperatures (16°C, 25°C, 30 °C or 37 °C as indicated) with shaking at 250 rpm in the MAXQ 4000 shaking incubator for protein expression. For protein expression at 16 °C or 25 °C, the culture was incubated at 37°C for 2 h and then at the indicated temperature overnight (approximately 14-16 h). For protein expression at 30 °C or 37 °C, the culture was incubated at the indicated temperature overnight (approximately 14-16 hours). 1 mL of bacterial culture was taken for centrifugation at 21,000 x g for 1 min with a Sorvall Legend Micro 21 centrifuge. The supernatant was discarded and the cell pellet was used for SDS-PAGE (see 2.3.4). Another 1 mL of bacterial culture was taken for cell lysis (see 2.3.3.1).

2.3.2.3. Auto-induction of recombinant VP3 with or without other proteins using LB-505

Auto-induction with LB-505 was performed based on published protocol¹⁵⁰. A colony of transformed *E. coli* (BL21(DE3)) from freshly streaked plates was picked to inoculate 3 mL or 25 mL of LB broth containing 1% (w/v) glucose and appropriate antibiotics (see Table 2.9 for details) depending on the scales of protein expression. The culture was incubated at 37°C overnight (approximately 14-16 h) with shaking at 250 rpm in the MAXQ 4000 shaking incubator. The next day, starter cultures of *E. coli* (BL21(DE3)) transformed with different plasmid vectors were used to inoculate LB-505 broth containing protein expression inducers and appropriate antibiotics (see Table 2.9 for details). For small-scale protein expression, 60 µL of starter culture was used to inoculate 3 mL of culture media in a 14 mL test tube. For larger-scale protein expression, 10 mL of starter culture was used to inoculate 500 mL of culture media in a 2 L Erlenmeyer flask. Cultures were incubated at different temperatures (16°C, 25°C, 30 °C or 37 °C as indicated) with shaking at 250 rpm in the MAXQ 4000 shaking incubator for protein expression. For protein expression at 16 °C or 25 °C, the culture was incubated at 37°C for 2 h and then at the indicated temperature overnight (approximately 14-16 h). For protein expression at 30 °C or 37 °C, the culture was incubated at the indicated temperature overnight (approximately 14-16 hours). 1 mL of bacterial culture was taken for centrifugation at 21,000 x g for 1 min with a Sorvall Legend Micro 21 centrifuge. The supernatant was

discarded and the cell pellet was used for SDS-PAGE (see 2.3.4). For small-scale expression, cell lysis was performed directly after expression (see 2.3.3.1). For larger-scale expression, the cells were collected by centrifugation at 4,600 x g for 10 min at 4 °C in TX-400 Swinging Bucket Rotor fitted into a Heraeus™ Multifuge™ X1R centrifuge. Supernatants were discarded and the cell pellets were stored at -80 °C.

Table 2.9 Plasmid vectors, antibiotics and and expression inducers used for auto-induction with LB-505

Target recombinant proteins	Vectors	Antibiotics	Expression inducers*
VP3	pET15b-ΔHis-VP3	100 μg/mL CAR	25 μM IPTG
VP3, AAP	pET15b-ΔHis-VP3-AAP	100 μg/mL CAR	25 μM IPTG
VP3, trigger factor	pET15b-ΔHis-VP3	100 μg/mL CAR	25 μM IPTG
	pTf16	25 μg/mL CHL	1 mg/mL arabinose
VP3, Hsp70	pET15b-ΔHis-VP3	100 μg/mL CAR	25 μM IPTG
	pKJE7	25 μg/mL CHL	1 mg/mL arabinose
VP3, Chaperonin	pET15b-ΔHis-VP3	100 μg/mL CAR	25 μM IPTG
	pGro7	25 μg/mL CHL	1 mg/mL arabinose
VP3, AAP, trigger factor	pET15b-ΔHis-VP3-AAP	100 μg/mL CAR	25 μM IPTG
	pTf16	25 μg/mL CHL	1 mg/mL arabinose
VP3, AAP, Hsp70	pET15b-ΔHis-VP3-AAP	100 μg/mL CAR	25 μM IPTG
	pKJE7	25 μg/mL CHL	1 mg/mL arabinose
VP3, AAP, Chaperonin	pET15b-ΔHis-VP3-AAP	100 μg/mL CAR	25 μM IPTG
	pGro7	25 μg/mL CHL	1 mg/mL arabinose

CAR=carbenicillin, CHL=chloramphenicol

*Final concentrations used after optimization testing

2.3.3. Cell lysis

2.3.3.1. Cell lysis protocol 1 (small-scale expression)

1 mL of bacterial culture was taken from the test tube after protein expression. The cells were collected by centrifugation at 21,000 x g for 1 min with a Sorvall Legend Micro 21 centrifuge. Supernatant was discarded and the pellet was resuspended in 100 µL of PBS. Then resuspended pellet was transferred to a 1.5-mL centrifuge tube fixed in place in ice water and disrupted by sonication with a Misonix Ultrasonic liquid processor Model # S-4000 (Qsonica, CT). The amplitude was set to 5, pulse-on time was set to 2 s, process time was set to 30 s (15 cycles), and pulse-off time was set to 10 s. The lysate was then centrifuged at 16,000 x g for 15 min at 4 °C in a VWR™ Galaxy 16D Digital microcentrifuge (VWR, PA). Both the supernatant and the pellet were collected.

2.3.3.2. Cell lysis protocol 2 (larger-scale expression)

Cell pellets stored at -80 °C were thawed on ice and then resuspended Purification Buffer A using 1/10th the volume of the culture media volume used for protein expression. 5 mL aliquots of resuspended pellet were transferred into 50 mL centrifuge tubes fixed in place in ice water for sonication. For sonication, the amplitude was set to 30, pulse-on time was set to 5 s, process time was set to 3 min (36 cycles), and pulse-off time was set to 20 s. The sonicated lysates were then transferred to clean 50 mL centrifuge tubes. The sonication

process was repeated approximately 5 times until all cell pellets were disrupted. Benzonase nuclease was added to the lysates at 50 U/mL. Lysates were incubated at room temperature with shaking at 120 rpm in the MAXQ 4000 shaking incubator for 40 min. 5 M NaCl stock solution was added to lysates to achieve a final concentration of 150 mM. Clarified lysates were prepared by centrifugation at 15,000 x g for 15 min at 4 °C in a Fiberlite™ F15-6 x 100y Fixed-Angle Rotor (Thermo Fisher Scientific, MA) fitted into a Heraeus™ Multifuge™ X1R centrifuge.

2.3.4. SDS-PAGE

2.3.4.1. Sample preparation and electrophoresis

For supernatants of the cell lysis, 5X SDS loading buffer was directly added into the samples so that the final concentration of loading buffer was 1X. For whole cells or pellets of the cell lysis, 80 µL of PBS was first used to resuspend the pellet and then 20 µL of 5X SDS loading buffer was added into the samples. All samples were mixed and incubated at 95 °C for 5 min. Self-made Bis-tris polyacrylamide gels (10% separating gels and 5% stacking gels) were used for electrophoresis in a VWR® Mini Vertical PAGE System (VWR, PA).

2.3.4.2. Polyacrylamide gel staining

Commassie blue R-250 or silver nitrate was used for visualization of the protein bands after electrophoresis. Silver nitrate staining was performed with Pierce™ Silver Stain Kit according to the manufacturer's manual. For Commassie blue staining, a quick staining method was used¹⁵¹. The gel was soaked in 100 mL of Commassie blue staining solution and microwaved for approximately 30 s to near boiling. The gel was then gently rotated with VWR® Analog Rocking Platform Shakers (VWR, PA) for 5 min. The Commassie blue staining solution was discarded and the gel was soaked in 100 ml of Commassie blue destaining solution. After microwaving the gel for 30 s, the gel was rotated in the rocking platform shakers until clear protein bands could be observed.

2.3.5. Western blot

All western blots were performed with wet-transferring method using VWR® Mini PAGE Electroblotting System (VWR, PA). After SDS-PAGE, the polyacrylamide gel was electroblotted onto 0.22 µm nitrocellulose membranes (Pall Corporation, NY) at 200 mA in an ice bath for 1 h 30 min using tris-glycine transfer buffer. To confirm the efficiency of transfer, membranes were soaked in Ponceau S staining solution for 10 s followed by soaking in the distilled water. The membrane was blocked with blocking solution for 1 h and incubated with antibody diluted in blocking solution for 1 h. For primary antibody

dilution, 1:1000 dilution was used for Anti-Adeno-associated virus (AAV), VP1/VP2/VP3, clone B1 and 1:2000 dilution was used for Anti-His-tag Antibody. The membrane was washed three times with TBST for 5 min, followed by incubation with secondary antibody diluted in blocking solution for 1 h. For secondary antibody dilution, 1:5000 dilution was used for both Peroxidase-conjugated Affinipure Goat anti-mouse IgG (H+L) and Goat anti-rabbit IgG (H&L) HRP conjugate. The membrane was washed three times with TBST for 5 min. Finally, detection was performed by incubating the membrane with Supersignal™ west pico PLUS chemiluminescent substrate for 1 min followed by visualization with a UVP BioSpectrum™ MultiSpectral Imaging System (UVP, LLC, Upland, CA) according to the manufacturer's instruction.

2.3.6. Dot blot

For each sample, 100 µL was blotted on 0.2 µm nitrocellulose membrane using Bio-Dot Microfiltration Apparatus (Bio-Rad Laboratories, CA) as per manufacturer's instruction. Membranes were then blocked with blocking solution for 30 min at room temperature. Then membranes were incubated with diluted primary antibodies for 30 min at room temperature. For primary antibody dilution, 1: 500 dilution was used for both Anti-Adeno-associated virus (AAV2), intact particles, clone A20 and Anti-Adeno-associated virus (AAV), VP1/VP2/VP3, clone B1. Membranes were then washed three time with TBST for 5 min. Membrane were incubated with diluted secondary antibodies for 30 min. For secondary antibody dilution, 1: 5000 dilution was used for Peroxidase-conjugated

Affinipure Goat anti-mouse IgG (H+L). This was followed by washing membranes three times with TBST for 5 min. Finally, membranes were incubated with Supersignal west pico PLUS chemiluminescent substrate for 1 min and imaged with UVP BioSpectrum™ MultiSpectral Imaging System.

2.3.7. Iodixanol gradient ultracentrifugation

Iodixanol gradient ultracentrifugation was performed as previously described^{109,152}. Four concentrations of iodixanol, 15% (w/v), 25% (w/v), 40% (w/v) and 60% (w/v), were used for separation in the ultracentrifugation. 25% (w/v) and 40% (w/v) iodixanol was prepared by diluting 60% (w/v) iodixanol in PBS-MK (low salt) to designated concentrations. 15% (w/v) iodixanol was prepared by diluting 60% (w/v) iodixanol in PBS-MK (high salt). 0.5% (w/v) phenol red was added to 25% (w/v) and 60% (w/v) iodixanol at the final concentration of 0.004% (w/v). To prepare layers of iodixanol with different concentrations, 6 ml of 15% (w/v) iodixanol, 6 ml of 25% (w/v) iodixanol, 5 mL of 40% (w/v) iodixanol, and 5 mL of 60% (w/v) iodixanol were sequentially added to a 32.4-mL OptiSeal Polypropylene tube (Beckman Coulter, NJ) with 2-mL serological pipettes. Clarified lysates were then gently overlaid onto the 15% (w/v) iodixanol layer with 10-mL syringes and filled up with PBS-MK (low salt) when necessary. Samples were centrifuged in a Type 70 Ti Fixed-Angle Titanium Rotor (Beckman Coulter, NJ) fitted in an Optima XE-90 ultracentrifuge (Beckman Coulter, NJ) at 63,100 rpm for 1 h 45 min at 10 °C. After centrifugation, the OptiSeal tube was punctured at the position slightly below the 60-40%

interface with a 16 g needle attached to a syringe. 25% (w/v) iodixanol and 40 % (w/v) iodixanol layers were collected by the syringe. The collected samples were stored at 4 °C until usage.

2.3.8. PEG precipitation

PEG precipitation was performed as previously reported¹⁰⁷. PEG stock solution was added to the protein sample to make the final concentration of PEG at 8% (w/v). After mixing, the sample was incubated at 4 °C for 1 -16 h. The precipitation was then collected by centrifugation at 3,000 x g for 15 min at 4 °C in Multifuge™ X1R centrifuge equipped with TX-400 Swinging Bucket Rotor. The supernatant was discarded, and the pellet was resuspended in an appropriate buffer dependent on the usage.

2.3.9. Triton X-114 phase separation

Triton X-114 phase separation was performed based on published protocol¹⁵³. Triton X-114 was added into protein samples to a final concentration of 1% (v/v). After mixing, samples were incubated on ice for 5 min followed by incubation at 37 °C for about 10 min until the lysate was turbid. Different phases of the protein samples formed after centrifugation at 15,000 x g for 10 min at room temperature in a Multifuge™ X1R centrifuge equipped with F15-6 x 100y Fixed-Angle Rotor. The aqueous phase (top phase) was transferred to another tube and saved for future use.

2.3.10. Polyethylenimine (PEI) protein precipitation

Precipitation of proteins with PEI was performed based on the published protocol¹⁵⁴. After Triton X-114 phase separation, PEI stock solution was added into the protein samples to a final concentration of 0.1% (v/v) then mixed well. The samples were incubated on ice for 5 min followed by centrifugation at 12,000 x g at 4 °C for 5 min in the MultifugeTM X1R centrifuge equipped with F15-6 x 100y Fixed-Angle Rotor. The supernatants were discarded, and the pellets were resuspended in buffer containing 20 mM Tris pH 8.5, 300 mM NaCl, 5 mM ATP, 0.001% Pluronic F-68. After incubation on ice for 5 min, the protein samples were centrifuged at 12,000 x g at 4 °C for 5 min and supernatant was collected.

2.3.11. Ammonium sulfate protein precipitation

Precipitation of proteins with ammonium sulfate was performed based on the published protocol¹⁵⁴. Saturated ammonium sulfate solution (approximately 4 M) was added to the samples to approximately 70% saturation. The samples were incubated at 4 °C overnight (approximately 14 -16 h) followed by centrifugation at 15,000 x g at 4 °C for 5 min in the MultifugeTM X1R centrifuge equipped with F15-6 x 100y Fixed-Angle Rotor. The supernatants were discarded, and the pellets were resuspended in the buffer dependent on the usage.

2.3.12. Protein purification by chromatography

All chromatographic protein purifications were performed using a BioLogic LP low-pressure chromatography system (Bio-Rad, CA) and fractions were collected using a BioFracTM Fraction Collector (Bio-Rad, CA). HiTrap Q XL (1 mL column), HiTrap Heparin HP (1 mL column) and Sephacryl S-300 HR resin were used for purification. Sephacryl S-300 HR resin was packed into an empty C 16/70 column (column I.D.: 16 mm, tube Height: 700 mm) per the manufacturer's instruction to achieve a bed volume of approximately 150 mL. Columns were equilibrated with equilibration buffers prior to sample loading. Protein samples were filtered with a syringe filter with 0.22 μm cellulose acetate membrane and 3 mL of protein sample was loaded into the sample loop. Fractions were collected based on running time. See Table 2.10 for details.

2.3.13. Transmission electron microscopy

Negative staining was performed based on as previously reported⁹⁹. The 300-mesh copper grid with formvar and carbon coatings was hydrophilized by UV irradiation in a Labconco Purifier Class II Biosafety Cabinet (Labconco Corporation, MO) for approximately 1 h. 3 μL of protein sample was placed on the grid for 60 s. The excess liquid was blotted and 5 μL of distilled water was placed on the grid to wash the grid. After blotting the excess liquid, 5 μL of UranylLess was placed on the grid for 60 s. The excess liquid was blotted

and the grid was dried for 5 min. The grid was examined using a JEOL JEM1200EX transmission electron microscope (Japan Electronic Optics Laboratory, MA) at 80 kV.

Table 2.10 Chromatographic conditions for protein purification

Column	Equilibration buffer	Time for each fraction collected	Running program			
			Step	Purification Buffer	Duration	Flow rate
HiTrap Q XL, 1 mL	Purification Buffer A	1 min	1	Buffer A	10 min	0.5 mL/min
			2	Buffer A	15-20 min	1 mL/min
			3	0 - 100% Buffer B	10 min	1 mL/min
			4	Buffer B	20-25 min	1 mL/min
HiTrap Heparin HP, 1 mL	Purification Buffer C	1 min	1	Buffer C	10 min	0.5 mL/min
			2	Buffer C	15-20 min	1 mL/min
			3	0 - 100% Buffer D	10 min	1 mL/min
			4	Buffer D	20-25 min	1 mL/min
Sephacryl S-300 HR, 150 mL, self-packed	Purification Buffer E	3 min	1	Buffer E	160 min	1 mL/min

See table 2.6 for buffer components and formulations.

CHAPTER 3 RESULTS

3.1. AAP promotes the assembly of VP3-only VLP in *E. coli*

It was previously reported by Le et al. that VP3 of AAV2 was largely found in inclusion bodies when expressed in *E. coli*¹⁰². They proposed that protein misfolding was likely responsible for VP3 aggregation in the inclusion bodies, and their study was based on refolded denatured VP3 isolated from inclusion bodies. Our goal, however, was to explore the possibility of expressing soluble VP3 in *E. coli*. To initiate our investigation, a modified pET-15b-based plasmid was constructed to express VP3 from AAV2 in *E. coli* (Figure 3.1a). The pET-15b- Δ His-VP3 expression vector was constructed with removal of the included His-tag, leaving expression of only native VP3 sequence. Recombinant VP3 from this vector was tested for expression by three methods: traditional IPTG-based protein expression in LB culture media, auto-induction in ZYP-5052 media¹⁴⁹ and auto-induction in LB-505 media¹⁵⁰ (see Table 2.2 for formulation and 2.3.2 for detailed methods). The auto-induction method was based on the catabolite repression caused by glucose to control the target protein expression in *E. coli*¹⁴⁹. Unlike the traditional IPTG-based method, only temperatures and media need to be optimized in auto-induction methods, and more consistent and replicable results can be obtained using auto-induction methods for protein expression.

All the expression conditions for recombinant VP3 are summarized in Table 3.1. It was observed in all conditions that the majority of recombinant VP3 expressed in *E. coli* was insoluble after cell lysis in agreement with the findings of Le et al.. A representative result using auto-induction with LB-505 at 30 °C (condition no. 15 in Table 3.1) is shown in Figure 3.2 (Figure 3.2a, Lanes 2&4 and Figure 3.2b, Lanes 1&3). However, a small fraction of soluble VP3 was detected after optimization of the expression conditions as shown in the representative result (Figure 3.2a, Lane 2 and Figure 3.2b, Lane 1). Using auto-induction with LB-505 media at 30 °C consistently demonstrated the highest production of soluble VP3 (condition no. 15 in Table 3.1). Other conditions listed in Table 3.1 did not demonstrate any significant improvements to solubility of recombinant VP3 (*data not shown*). The auto-induction method with LB-505 media at different temperatures was used subsequently unless otherwise stated. Although expression using LB-505 at different temperatures did not produce high yields of soluble VP3, LB-505 was chosen for ease-of-use and no improvement upon LB-505 media was observed for other media investigated here.

Table 3.1 Expression conditions tested for expression of recombinant VP3.

Condition no.	Medium	Concentration of IPTG	Temperature	Time of expression
1	LB	0.1 mM	16 °C	~ 14-16 h
2	LB	1 mM	16 °C	~ 14-16 h
3	LB	0.1 mM	25 °C	~ 14-16 h
4	LB	1 mM	25 °C	~ 14-16 h
5	LB	0.1 mM	30 °C	~ 6 h
6	LB	1 mM	30 °C	~ 6 h
7	LB	0.1 mM	37 °C	~ 6 h
8	LB	1 mM	37 °C	~ 6 h
9	ZYP-5052	-	16 °C	~ 14-16 h
10	ZYP-5052	-	25 °C	~ 14-16 h
11	ZYP-5052	-	30 °C	~ 14-16 h
12	ZYP-5052	-	37 °C	~ 14-16 h
13	LB-505	0.025 mM	16 °C	~ 14-16 h
14	LB-505	0.025 mM	25 °C	~ 14-16 h
15	LB-505	0.025 mM	30 °C	~ 14-16 h
16	LB-505	0.025 mM	37 °C	~ 14-16 h

Auto-induction used for conditions 9-16.

Concurrent with efforts to optimize the expression of recombinant VP3 in *E. coli*, the capsid formation potential of VP3 was also assessed. Prior evidence has suggested that AAV2 capsids were not able to self-assemble during expression of VP3 alone in *E. coli*^{60,155}. An immunological detection assay (dot blot) was used to indicate the presence of potential VP3-only capsids with two different clones of anti-AAV2 monoclonal antibodies¹⁵⁶. The monoclonal A20 antibody preparation has been demonstrated to detect the intact capsid of AAV2 as the epitope recognized by A20 is only present within intact capsids. On the other hand, the monoclonal B1 antibody preparation detects VP3 as part of denatured capsids or unassembled VP3 since it interacts with an epitope that is inaccessible in the native capsids. As shown in Figure 3.2c, after expression of recombinant VP3 using Condition no. 15 in Table 3.1, clarified cell lysates incubated with A20 antibodies were unable to detect the presence of capsids (Figure 3.2c, Column 1), but incubation with B1 antibodies produced a strong signal indicating the presence of soluble VP3 (Figure 3.2c, Column 1). Similarly, for clarified lysates after expression using all conditions listed in Table 3.1, capsid assembly in *E. coli* by VP3 was not detected. These findings suggested that intact capsids were unable to form when recombinant VP3 was expressed alone in *E. coli*. Furthermore, it was likely that the soluble VP3 detected after expression was present in monomeric or oligomeric states.

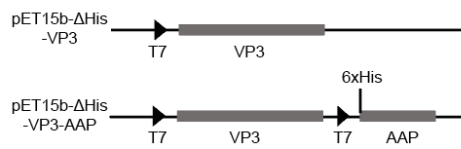
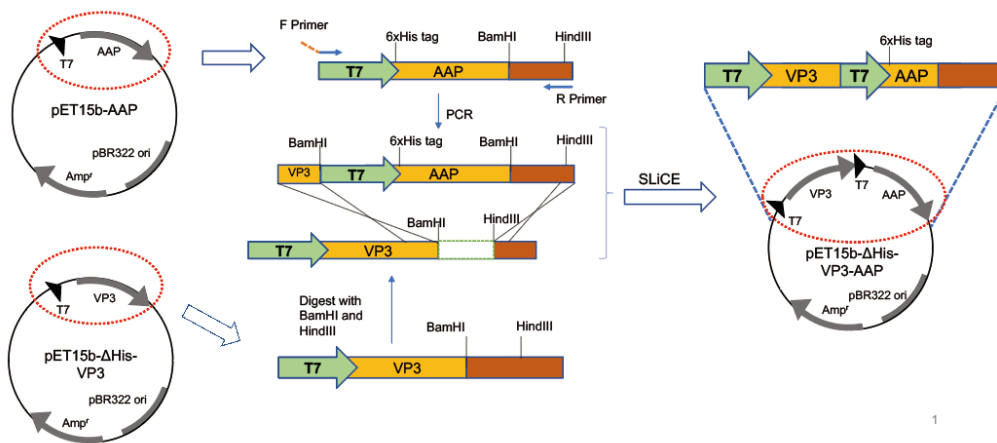
A**B**

Figure 3.1 Expression vector plasmids: target protein expression of VP3 or co-expression of VP3 and AAP. (A) Schematic of expression vectors. Promoters and target recombinant proteins indicated (B) Schematic of the construction of pET15b-ΔHis-VP3-AAP (see Materials and Methods for details).

It has been proposed that AAV2 is an AAP-dependent virus, where capsid assembly is dependent upon the assistance of AAP¹⁵⁵. In human cells, VP3-only capsid of AAV2 was formed when VP3 was co-expressed with AAP⁶⁰. Le et al. (2022) have also demonstrated that AAP can promote AAV5 capsid assembly in *E. coli*¹⁰¹. Therefore, we investigated the potential dependency of VP3 upon AAP for capsid assembly when expressed as a recombinant protein in *E. coli*. To test this hypothesis, VP3 and AAP were co-expressed in *E. coli* by inserting the coding sequences of VP3 and AAP in the same plasmid vector and under the control of different T7 promoters to create the dual expression vector pET-15b-ΔHis-VP3-AAP (Figure 3.1b). Co-expression of VP3 and AAP was first tested at 30 °C with LB-505 culture media. The successful co-expression of VP3 and AAP was detected by SDS-PAGE analysis and immunoblotting analysis (Western blotting) using anti-AAV2, clone B1 (Figure 3.2a, Lanes 3 & 5 and Figure 3.2b, Lanes 2 & 4). However, both soluble (Figure 3.2b, Lane 2) and insoluble (Figure 3.2b, Lane 4) protein levels of VP3 were lower after co-expression compared to soluble (Figure 3.2b, Lane 1) and insoluble (Figure 3.2b, Lane 3) levels of VP3 after expression of VP3 alone. Next, dot blot assays were performed to examine the potential formation of capsids by VP3 after co-expression with AAP. The presence of VP3-only capsids was detected when co-expressing VP3 and AAP at 30 °C, since A20 antibodies were able to detect epitopes of intact capsids after co-expression (Figure 3.2c, Column 2). Furthermore, analogous assays performed with co-expression at 16 °C, 25 °C and 37°C did not demonstrate the production of VLP (*data not shown*).

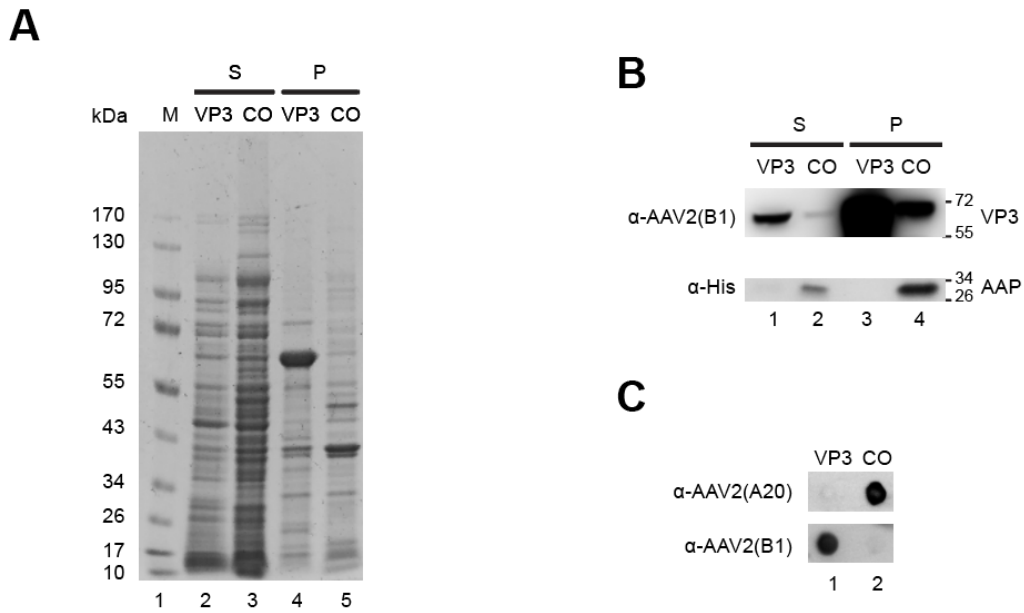


Figure 3.2 Expression of VP3 and co-expression of VP3 and AAP in *E. coli* using auto-induction method with LB-505 at 30 °C for approximately 14-16 h. (A) SDS-PAGE gel stained with Coomassie blue R-250. Lane 1: protein molecular weight marker with apparent molecular weight in kDa. Lane 2 & 3: soluble (Lane 2) and insoluble (Lane 3) proteins of cell lysates after expression of VP3 alone. Lane 4 & 5: soluble (Lane 4) and insoluble (Lane 5) proteins of cell lysates after co-expression of VP3 and AAP. (B) Western blot detection using B1 antibody. Lane 1–4: samples corresponding to Lane 2–5 of (A). (C) Dot blot assay using B1 and A20 antibodies. Column 1: supernatant of cell lysates after expression of VP3 alone. Column 2: supernatant of cell lysates after co-expression of VP3 and AAP. Abbreviations in all panels indicate: "M" = protein apparent molecular weight marker. "S" =supernatant of protein samples after extraction. "P" = pellets of protein samples after extraction. "VP3" = protein expression of VP3 alone. "CO" = VP3 and AAP protein co-expression.

3.2. Characterization of VP3 by Transmission Electron Microscopy

To further investigate the expressed VP3 after co-expression with AAP we conducted transmission electron microscopy (TEM). The clarified lysates after co-expression of VP3 and AAP at 30 °C with LB-505 were enriched by iodixanol gradient ultracentrifugation (see 2.3.7 for details) and PEG precipitation (see 2.3.8 for details) and negative stained for TEM detection (see 2.3.13 for details). Using TEM, capsid-like structures were observed as indicated in Figure 3.3. These observed structures were in support of the formation of VP3-only VLPs in *E. coli* upon co-expression of VP3 with AAP. It should be noted that under the conditions tested, only a very low titer was achieved.

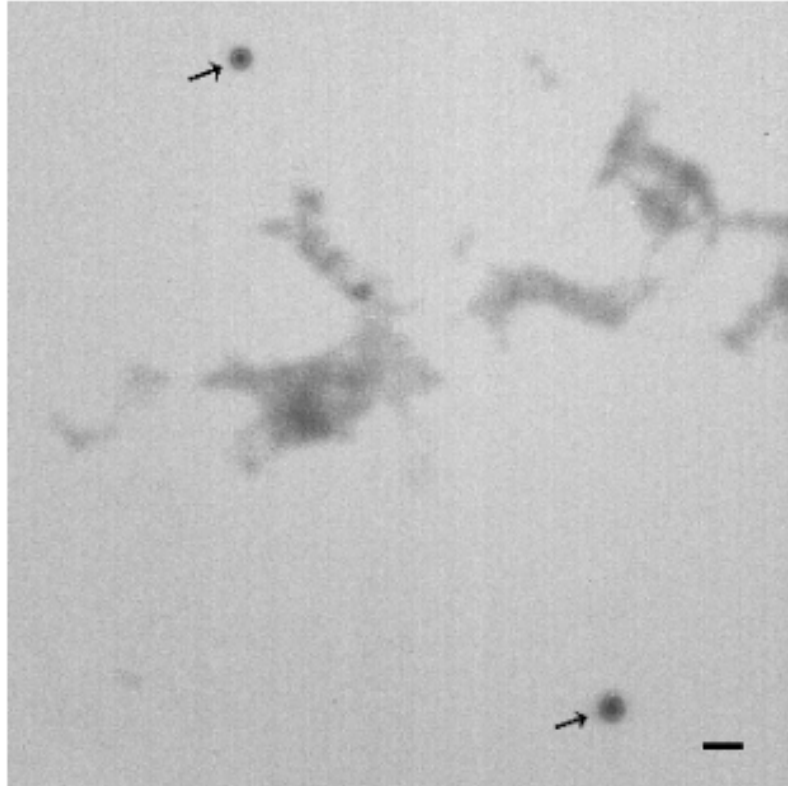


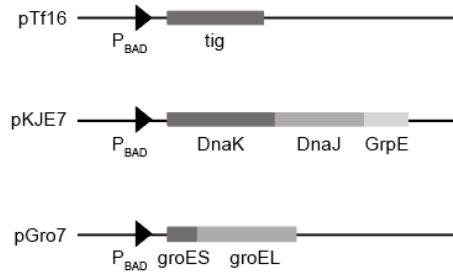
Figure 3.3 Characterization of VP3 by transmission electron microscopy with negative staining. Enriched protein samples from clarified lysates of co-expression of VP3 and AAP with auto-induction in LB-505 media at 30 °C were used for observation. Arrows indicate the capsid-like structures detected. The scale bar represents 100 nm.

3.3. Co-expression of different chaperones with VP3 promotes soluble expression and assembly of VP3 in *E. coli*

Next, we wanted to explore potential ways to increase VP3-only VLP production in *E. coli*. Although the dot blot analysis indicated that almost all soluble recombinant VP3 after co-expression with AAP self-assembled and only interacted with antibody A20 (Figure 3.2c, Column 2), the overall protein level of soluble VP3 after co-expression of VP3 and AAP (Figure 3.2b, Lane 2) decreased compared to that level after expression of VP3 alone (Figure 3.2b, Lane 1). In other words, the presence of AAP seemed to increase the solubility of VP3 and promote the assembly of VP3-only VLP at the expense of the total expression levels of VP3. Therefore, we sought to investigate conditions with both increased solubility and increased yield. Replacement of AAP with other proteins with similar potential functions as AAP were investigated. It was suggested that AAP may serve as a chaperone during AAV capsid assembly⁸⁴. Thus, we speculated that other chaperones, when co-expressed with VP3, might promote capsid assembly and increase the overall protein level of VP3. To test this hypothesis, co-expression of VP3 with different chaperones from *E. coli* (trigger factor, Hsp70 and chaperonin) was conducted. The co-expression was achieved by transforming *E. coli* with two plasmids (Figure 3.4b, see 2.3.2.3 for details), one expressing VP3 and the other expressing chaperones (Figure 3.4a). Three plasmids were used for the expression of chaperones: pTf16 vector for the expression of trigger

factor, pKJE7 for the expression of Hsp70 system and pGro7 for the expression of chaperonin system.

A



B

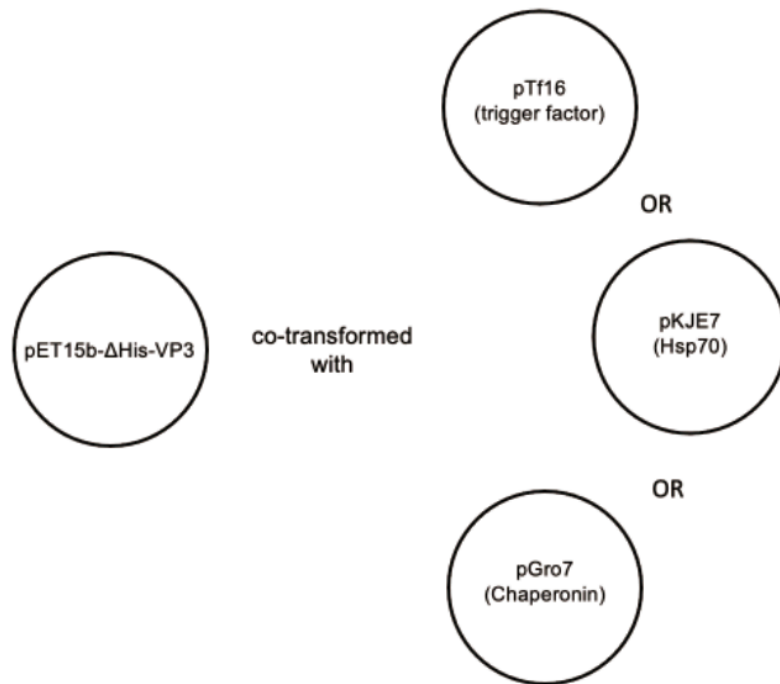


Figure 3.4 Expression vector plasmids: co-expression of VP3 with different chaperones. (A) Schematic of expression vectors of chaperones. Promoters and target recombinant proteins indicated. (B) Schematic of strategies of co-expression of chaperones and VP3.

Co-expression of VP3 and chaperones was first performed at 30 °C using LB-505 culture media. All chaperones investigated increased the soluble expression of VP3 (Figure 3.5b, Lanes 2-4) compared to expression of VP3 alone (Figure 3.5b, Lane 1). The chaperones also decreased the presence of insoluble VP3 (Figure 3.5b, Lanes 6-8) compared to VP3 expression alone (Figure 3.5b, Lane 5). However, dot blot analysis demonstrated that increased proportion of soluble VP3 did not form capsids, as the majority of protein was detected using the B1 monoclonal antibodies (Figure 3.5c, Columns 2-4). Clarified lysates from co-expression of VP3 and trigger factor (Figure 3.5c, Column 2) or co-expression of VP3 and chaperonin (Figure 3.5c, Column 4) showed very weak signal using the A20 monoclonal antibodies. This implied that trigger factor and chaperonin had very little impact on promoting capsid assembly of VP3 (Figure 3.5c, Columns 2 & 4). Co-expression of chaperones and VP3 at different temperatures (16 °C, 25 °C or 37 °C) with LB-505 culture media was also tested, but co-expression under those conditions did not demonstrate any improvement in capsid-like particle production (*data not shown*). Thus, co-expression of VP3 and chaperones from *E. coli* (trigger factor, Hsp70 and chaperonin) promoted VP3 soluble expression, but only trigger factor and Hsp70 had a small effect on capsid assembly of VP3.

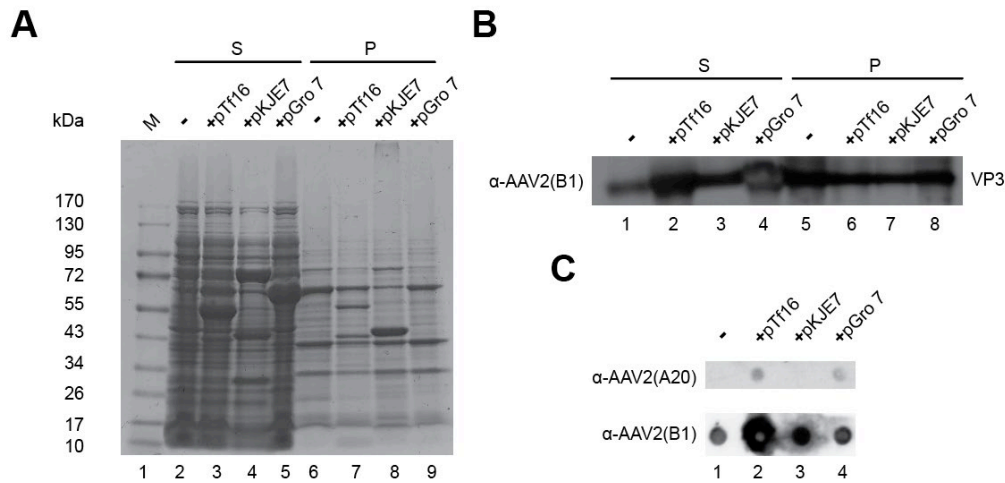


Figure 3.5 Co-expression of VP3 with different chaperones in *E. coli* at 30 °C. (A) SDS-PAGE gel stained with Coomassie blue R-250. Lane 1: protein molecular weight marker with apparent molecular weight in kDa. Lanes 2-9: soluble (Lane 2-5) and insoluble (Lanes 6-9) proteins of cell lysates after expression or co-expression as indicated. (B) Western blot detection using B1 antibody. Lane 1–8: samples corresponding to Lanes 1–8 of (A). (C) Dot blot assay using B1 and A20 antibodies. Columns 1-4: samples corresponding to Lanes 2–5 of (A). Abbreviations in all panels indicate: "-" = VP3 expression alone. "+" = VP3 co-expressed with chaperones encoded by indicated plasmids. "M" = protein apparent molecular weight marker. "S" = supernatant of protein samples after extraction. "P" = pellets of protein samples after extraction.

3.4. Chaperonin increased assembled VP3 production in *E. coli* when co-expressed with VP3 and AAP

To further improve VP3-only VLP production in *E. coli*, the expression of VP3 along with AAP and *E. coli* chaperones simultaneously was studied. This co-expression was accomplished by co-transformation of the pET15b- Δ His-VP3-AAP and one of the chaperone-expressing vectors (Figure 3.6a, see 2.3.2.3 for details). Co-expression cultures of the dual expression pET15b- Δ His-VP3-AAP vector along with one of the chaperone-expressing vectors were each performed at different temperatures, 16 °C, 25 °C, 30 °C or 37 °C, in LB-505 culture media. Only the cleared cell lysate (soluble fraction) was investigated using both the B1 and A20 monoclonal antibodies to assess for the potential formation of VP3-only VLPs. For co-expression at 16 °C or 25 °C, no capsid formation was detected using the dot blot assay with A20 antibody for all three *E. coli* chaperones (*data not shown*). At 30°C, trigger factor and chaperonin only slightly enhanced assembled VP3 production when co-expressed with VP3 and AAP (Figure 3.6b, Columns 2 & 4) compared to co-expression of VP3 and AAP without any chaperones (Figure 3.6b, Column 1). Unexpectedly, chaperonin could increase assembled VP3 production at 37 °C when co-expressed with VP3 and AAP (Figure 3.6b, Column 4), while there were no assembled VP3 detected when co-expressing VP3 and AAP without chaperones (Figure 3.6b, Column 1). Taken together, the results suggest that chaperonin promoted VP3-only VLP production in

E. coli when co-expressed with AAP and VP3 at 30 °C and 37 °C, with potentially greater production at 37 °C.

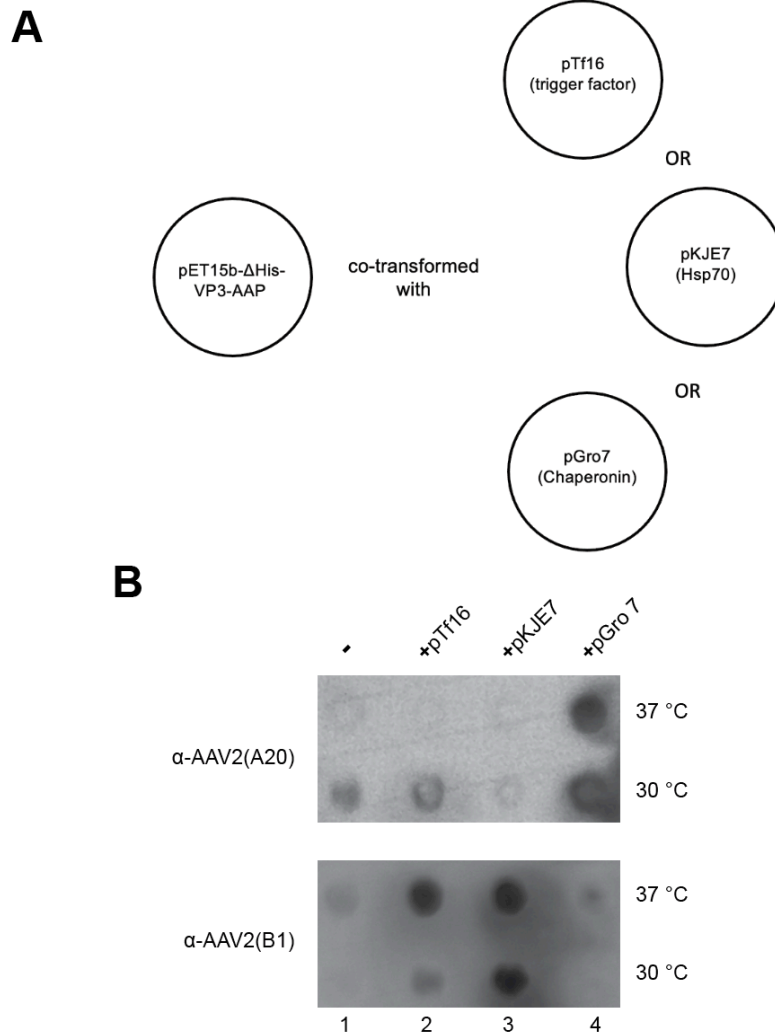


Figure 3.6 Triple co-expression of VP3 and AAP with different chaperones. (A) Schematic of strategies of triple co-expression of VP3, AAP and chaperones. (B) Dot blot assay of expressed protein samples. The temperature indicated the temperature applied to perform protein expression. Abbreviations in all panels indicate: "-" = VP3 and AAP co-expression. "+" = VP3 and AAP co-expressed with chaperones encoded by indicated plasmids.

3.5. Purification of VP3-only Virus-Like Particles

With the apparent increased efficiency in production of VLPs under triple co-expression of VP3, AAP and chaperonin in *E. coli*, purification of the VLPs was attempted using *E. coli* after triple co-expression at 37 °C with LB-505 culture media. For the preparation of cell lysate for purification, the cell lysis methods that have been used for AAV2 purification were adopted with adaptations (see 2.3.3.2 for details)¹⁵⁷. It was reported that AAV2 virus could associate with contaminants like nucleic acids and endotoxins that would impact purification^{158,159}. Therefore, Bezonase nuclease digestion¹⁵⁷ and Triton X-114 phase separation¹⁵³ were applied to remove nucleic acids and endotoxins separately as pre-treatment before attempted purification.

Several purification techniques commonly used in AAV2 virus purification have been tried for VP3-only VLP purification¹⁶⁰. First, affinity-column purification was attempted using a 1 mL HiTrap Heparin HP column with 3 mL clarified lysates after pre-treatment (see 2.3.12 for detailed procedure). Dot blot assays using A20 monoclonal antibodies was used to assay for the presence of VLPs in collected fractions during purification, and the results indicated that fractions 51-56 contained VP3-only VLPs (Figure 3.7c). However, after SDS-PAGE and silver nitrate staining, the results indicated those fractions still contained many non-target proteins in addition to VP3 (Figure 3.7b, Lanes 8-11). Since the overall concentrations of proteins from fractions 51-56 were low after purification (Figure 3.7b,

Lanes 8-11), further purification steps were unlikely to produce usable quantities of protein, and an alternative to Heparin resin was selected. Anion exchange chromatography has also been widely used for AAV2 purification¹⁶⁰. Thus, we applied a 1 mL HiTrap Q XL column (pre-packed with strong anion exchanger Q) for VP3-only VLP purification from 3 mL pf processed lysates. However, the result demonstrated that most VP3-only VLP did not bind to the Q column and remained in the fractions of flow-through (fraction no. 8) (Figure 3.8b, Lane 3 and Figure 3.8c). Varying of the pH (7.5, 8 or 9) and the concentration of NaCl (0 mM, 30 mM NaCl or 50 mM NaCl) for equilibrium buffers for purification using Q column did not improve results (*data not shown*).

This phenomenon that VLP-like particles did not bind to Q column even at high pH and low ionic strength suggested that there might be aggregation or non-specific interactions between VP3 and other proteins, which interfered with the interaction between VLP and the Q column. In addition, it was observed chaperonin or GroEL was likely the major contaminating proteins during previous purification experiments (Figure 3.7b, Lane 3 and Figure 3.8b, Lane 3). To minimize the influence of chaperonin upon purification of VP3-only VLPs, a purification strategy was developed that combined PEI precipitation followed by size-exclusion chromatography (SEC). PEI is a basic cationic polymer and is positively charged in solutions of neutral and basic pH¹⁵⁴. It can be seen as an alternative to anion exchange chromatography with lower resolution but higher flexibility. The PEI precipitation was used to enrich VP3-only VLPs in the processed lysates (see 2.3.10 for

details). After PEI precipitation, ammonium sulfate precipitation was performed to concentrate protein samples and remove residual PEI in the samples. SEC was then conducted followed by ammonium sulfate precipitation. For SEC, a self-packed Sephacryl S-300 HR column with diameter of 16 mm and bed volume of 150 mL was used. 2.5 M urea was included in all buffers used for SEC purification based on the finding that chaperonin is dissociated into monomers at 2.5 – 3 M urea^{161,162}, while the capsid of parvovirus, like AAV2, can remain stable in this condition⁷⁵. Therefore, VP3-only VLPs and monomers of chaperonin could potentially be separated in the buffers containing urea due to their differences in size. The results indicated that VP3-only VLPs, detected by dot blot with A20 antibody (Figure 3.9c), were eluted in the void volume of the column (fraction no. 21-24, Figure 3.9a). In an attempt to obtain better purity, fractions no. 21-24 after SEC were applied to the Heparin column for purification. However, it appeared that the recovery of proteins after this step was extremely low as indicated by the very weak bands after silver nitrate staining of the SDS-PAGE gel (Figure 3.10b, Lanes 4-7). Therefore, no further purification steps were pursued at this time. Taken together, PEI combined with size-exclusion chromatography could be used to achieve a degree of purification of VP3-only VLPs, albeit at very low titer.

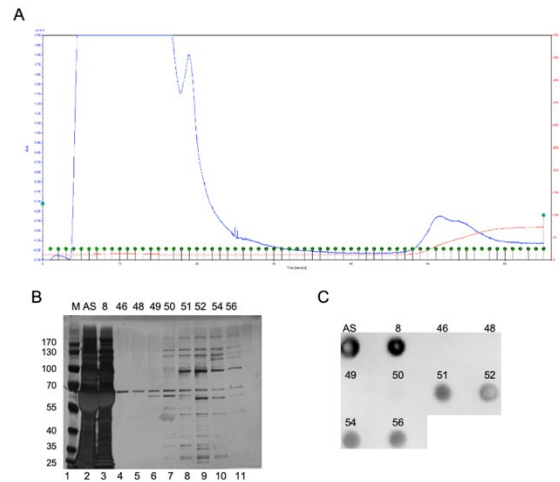


Figure 3.7 Chromatography of VP3-only VLPs with Heparin column. (A) Chromatogram of fractions collected. The blue line indicates the UV absorbance at 260 nm, and the red line indicates the ionic strength (approximately 0.15 - 1 M NaCl). Green marker points indicate points of fraction collection. (B) SDS-PAGE gel stained with silver nitrate. Lane 1: protein molecular weight marker with apparent molecular weight in kDa. Lane 2: protein sample after ammonium sulfate precipitation. Lanes 3-11: protein samples from indicated fraction numbers (C) Dot blot using A20 antibody. Abbreviations in all panels are: "M" = protein apparent molecular weight marker. "AS" = protein sample after ammonium sulfate precipitation.

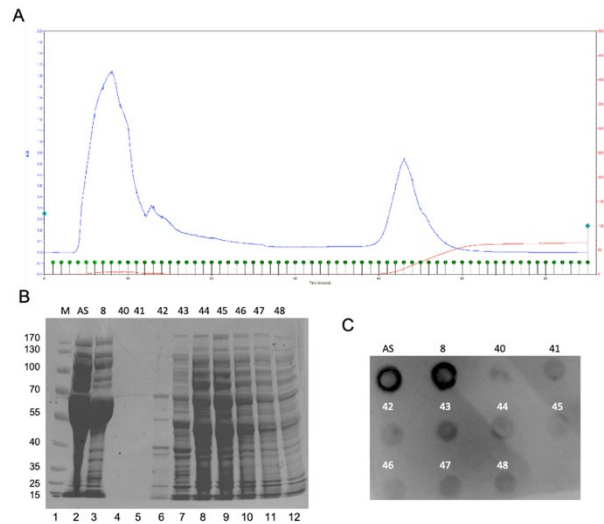


Figure 3.8 Chromatography of VP3-only VLPs with Q XL column. (A) Chromatogram of fractions collected. The blue line indicates the UV absorbance at 260 nm, and the red line indicates the ionic strength (approximately 0 - 1 M NaCl). Green marker points indicate points of fraction collection. (B) SDS-PAGE gel stained with silver nitrate. Lane 1: protein molecular weight marker with apparent molecular weight in kDa. Lane 2: protein sample after ammonium sulfate precipitation. Lanes 3-11: protein samples from indicated fraction numbers (C) Dot blot using A20 antibody. Abbreviations in all panels are: "M" = protein apparent molecular weight marker. "AS" = protein sample after ammonium sulfate precipitation.

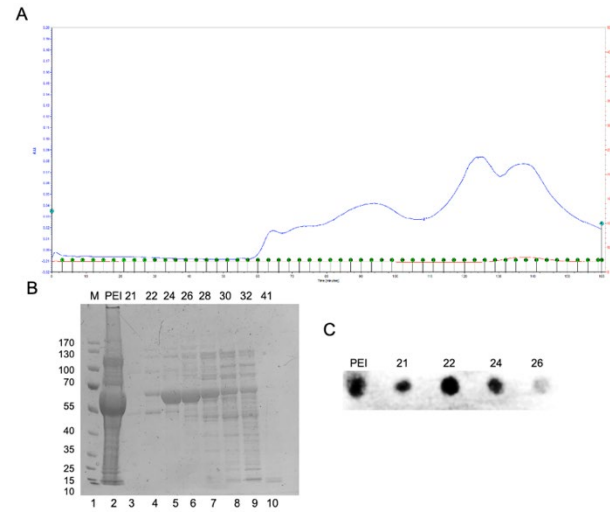


Figure 3.9 Chromatography of VP3-only VLPs with Sephacryl S-300 HR column. (A) Chromatogram of fractions collected. The blue line indicates the UV absorbance at 260 nm, and the red line indicates the ionic strength (approximately 0.45 M NaCl). Green marker points indicate points of fraction collection. (B) SDS-PAGE gel stained with silver nitrate. Lane 1: protein molecular weight marker with apparent molecular weight in kDa. Lane 2: protein sample after ammonium sulfate precipitation. Lanes 3-11: protein samples from indicated fraction numbers (C) Dot blot using A20 antibody. Abbreviations in all panels are: "M" = protein apparent molecular weight marker. "PEI" = protein sample after PEI precipitation and ammonium sulfate precipitation.

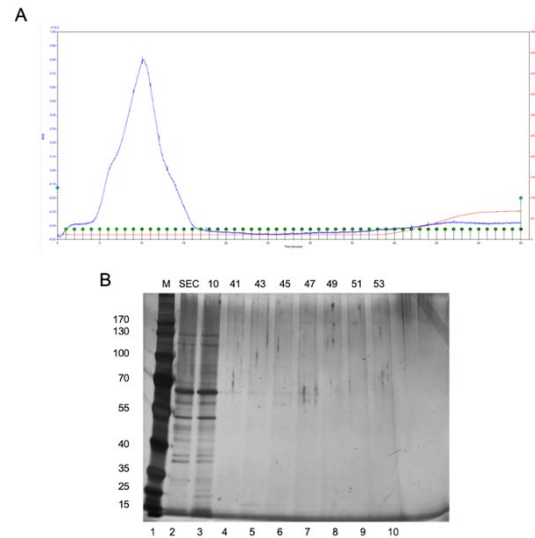


Figure 3.10 Chromatography of VP3-only VLPs with Heparin column (polishing). (A) Chromatogram of fractions collected. The blue line indicates the UV absorbance at 260 nm, and the red line indicates the ionic strength (approximately 0.15 - 1 M NaCl). Green marker points indicate points of fraction collection. (B) SDS-PAGE gel stained with silver nitrate. Lane 1: protein molecular weight marker with apparent molecular weight in kDa. Lane 2: protein sample after ammonium sulfate precipitation. Lanes 3-11: protein samples from indicated fraction numbers. Abbreviations in all panels are: "M" = protein apparent molecular weight marker. "SEC" = protein sample after SEC purification.

CHAPTER 4 DISCUSSION

4.1. Summary

AAV is a widely used vector in gene therapy¹⁶³. However, few studies have focused on developing capsids or VLPs of AAV for other applications. One of the reasons is the high cost of production of VLPs of AAV in eukaryotic cells⁹⁸. In this project, we explored the possibilities for production of VP3-only VLPs of AAV2 in *E. coli*, a prokaryotic protein expression system which is inherently associated with lower potential costs for production.

We first studied the expression of VP3 of AAV in *E. coli* under different expression conditions. Based on the extent of studies presented here, recombinant VP3 was not found to self-assemble into VP3-only VLPs in *E. coli*, although an increased amount of soluble VP3 expression was achieved. (Figure 3.2). Further studies demonstrated that AAP promoted VP3 assembly into VLPs in *E. coli* when VP3 and AAP were co-expressed in *E. coli* (Figure 3.2 and Figure 3.3). However, AAP, when co-expressed with VP3, seemed to compromise the expression levels of VP3 (Figure 3.2). In addition, although *E. coli* chaperones, namely trigger factor, Hsp70 and chaperonin, could improve soluble expression of VP3 when co-expressed with VP3, they could not replace AAP for promoting capsid assembly of VP3 (Figure 3.5). Trigger factor or chaperonin had a small effect on promoting VP3 capsid assembly, while for Hsp70, no effect on promoting VP3 capsid

assembly was detected (Figure 3.5). Interestingly, when triple co-expression of AAP, VP3 and Hsp70 was performed, Hsp70 inhibited the capsid formation compared to co-expression of AAP and VP3 at 30 °C (Figure 3.6). Triple co-expression of VP3, AAP and chaperonin at 30 °C or 37 °C could promote VP3-only VLP production compared to only co-expression of VP3 and AAP at the same temperatures (Figure 3.6). VP3-only VLP purification was also attempted using lysates from triple co-expression of VP3, AAP and Chaperonin at 37 °C. However, the purification achieved was marginal at best due to the low concentration of VP3-only VLPs in the lysates (Figures 3.7 to 3.10).

4.2. Impact of expression conditions on expression of recombinant VP3 in *E. coli*

In our project, many expression conditions for expression of VP3 alone were tested. Factors like temperatures (16 °C, 25 °C, 30 °C or 37 °C), expression methods (tradition IPTG-based or Auto-induction), and media (LB, ZYP-5052 and LB-505) were optimized in our experiments. However, many other factors may also play roles in expression of VP3 alone¹⁶⁴. For example, the promoter and the inducer used for protein expression may influence the expression of VP3. In our study, the strong promoter T7 was used for protein expression. A weaker promoter like the *lac* promoter might provide better results for protein expression since most expressed VP3 using T7 was found in inclusion bodies after expression (Figure 3.2), which implied that the expression of VP3 may be too robust leading to aggregation. Expression of VP3 with a weaker promoter might lower the expression rate, preventing the formation of inclusion bodies.

Moreover, other culture additives that affect the metabolic and growth rates of *E. coli*, like glycerol or sucrose, could be added into the culture media during protein expression. Future studies should include continued investigation of variable culture conditions for expression of VP3 alone, or in conjunction (co-expression) with other protein factors. Also, only the auto-induction method with LB-505 culture media was used in the experiments for co-expression of VP3 and other proteins. As is mentioned in the results (see 3.1), this was due to our findings that the variations caused by culture media were not significant. However, we cannot rule out the possibility that the variations may become remarkable when other factors, like culture additives, are included for optimization tests of protein expression in the future. Taken together, more comprehensive and more sophisticated strategies may be needed in the future for optimization of expression of recombinant VP3 in *E. coli*.

4.3. Impact of AAP on capsid assembly and protein expression of VP3 in *E. coli*

Previous research has demonstrated that the capsid assembly process of AAV2 required the participation of AAP in human cells as well as insect cells^{60,84}. Our study also showed that the assembly of VP3-only VLPs of AAV2 in *E. coli* required AAP.

In this study, the co-expression of AAP and VP3 was achieved using one plasmid. The expressions of these two proteins are controlled by their own promoters though the promoter sequences and ribosome binding sequences (RBS) controlling the expression of

these two proteins were the same. Co-expression using this method has several advantages. First, there was an ease of construction, since all cloning procedures of the co-expression plasmid were based on the plasmids that were easily accessible due to prior construction in-house. Second, no additional inducers were required for co-expression. Third, triple or even quadruple co-expression of AAP, VP3 and other proteins can be conducted by co-transformation of this co-expression plasmid with other plasmids. However, the major limitation of this co-expression method was that the relative levels of VP3 and AAP after co-expression are not adjustable independently of each other since the expression of these two proteins are controlled by the same inducers and promoters with the same sequences. As our results showed that AAP compromised the level of VP3 expression during co-expression of AAP and VP3, it may be important to control relative expression levels of AAP and VP3 independently. Future studies may include the development of new expression vectors allowing for independent control of AAP and VP3 expression levels.

Another interesting finding was that VP3-only VLPs could only be detected during co-expression of AAP and VP3 at 30 °C or co-expression of AAP, VP3 and chaperonin at 30 °C or 37 °C. This may suggest that *in situ* capsid assembly of AAV2 in *E. coli* may only occur during culture in a specific temperature range. In addition, AAP could potentially be mediating other mechanisms, such as protein degradation, during capsid assembly. AAP compromised the expression of VP3 when co-expressing VP3 and AAP in *E. coli* and the

dot blot assays using B1 antibody indicated there were nearly no monomers or aggregates of VP3 in the clarified cell lysates from co-expression of VP3 and AAP.

4.4. Impact of *E. coli* chaperones on capsid assembly and protein expression of VP3 in *E. coli*

In our project, it was confirmed that *E. coli* chaperones (trigger factor, Hsp70 and chaperonin) promoted soluble expression of VP3 when co-expressed (Figure 3.5). As these three chaperone systems work in different ways to help protein folding¹³⁴, it can be deduced from the results that the VP3 aggregation is possibly due to inefficient folding of the newly synthesized proteins in *E. coli* under the expression conditions tested here. Another potential cause of VP3 aggregation could be that VP3 monomers were not stable and could associate with other substances, such as other bacterial cell proteins and/or DNA. Chaperones used here are presumed to act under their normal function and bound to VP3, thus preventing interaction with other substances. However, those chaperones demonstrated little effect on promoting VP3 self-assembly. This could indicate that other potential mechanisms involving the participation of AAP to guide the process of capsid assembly were necessary. Interestingly, as Hsp70 demonstrated a negative effect on the assembly of VP3 in the presence of AAP, it could also be that the point of interaction of VP3 with Hsp70 is critical for capsid assembly of VP3.

It is reported that VP3 was able to assemble *in vitro* and form VP3-only VLP under specific conditions without the help of AAP¹⁰². Our results also demonstrated that trigger factor and chaperonin had little effect on promoting VP3-only VLP formation in *E. coli*. Based on the general theory of capsid assembly of viruses¹⁶⁵, it is likely that the assembly process of AAV2 is still a thermodynamic process, and AAP somehow improves the tendency of VP3 to assemble rather than aggregate. When there is no AAP, the assembly of VP3 is still a potential outcome, however, the thermodynamically preferred process is aggregation.

4.5. Practical consideration for purification of VP3-only VLP

Robust purification of VP3-only VLPs was not achieved. This was a significant challenge in this study due to the low level of VP3-only VLP production. It was estimated that more than 10 L of bacterial cultures might be needed based on the current yield. Nevertheless, the purification workflow developed in this study did result in the partial purification of immunologically detectable VLPs. Thus, the purification procedure may act as proof-of-concept for further optimization and refinement if additional future studies are able to address the level of production.

A second consideration for the development of purification strategies was the potential interference of chaperonin. The GroEL monomer has a molecular weight of ~60 kDa, which is close to the molecular weight of the VP3 monomer which created challenges for the separation and distinction of these co-expressed recombinant proteins. Future

purification strategies also need to address the apparent tight association of chaperonin with VP3.

4.6. Future directions

Our results have demonstrated that AAV2-based VP3-only VLPs can be produced in *E. coli*. However, the yield of VLP produced was extremely low. What will be needed is further exploration of expression conditions to 1) increase the soluble proportion of protein and/or 2) increase the *de novo* assembly of VLPs *in situ* during VP3 expression. In addition, other prokaryotic protein expression systems, like *Bacillus subtilis*, can be explored for VP3 expression.

Our next goal is to express VP1, VP2, and VP3 at the same time to produce native-like AAV2 VLPs. The results obtained here with VP3-only VLPs of AAV2, and potential results of studies including VP1 and VP2 could also be used as a point to initiate similar studies of other AAV serotypes as well. Of particular interest would be to explore 1) those serotypes that have not demonstrated an AAP dependency, like AAV5¹⁶⁶, and 2) other parvoviruses with similar structures as AAV2 in addition to AAV, like parvovirus B19¹⁶⁷.

In addition to the low yield of expressed VLPs in this study, another complicating factor impacting the purification attempts was likely the association between VP3 and chaperonin.

Although it may not be possible to directly reduce the interaction between VP3 and

chaperonin, some methods could potentially be used in the future to circumvent it. For example, co-expression VP3 with truncated GroEL (the core chaperone of chaperonin) instead of full-length GroEL or the addition of an affinity tag to GroEL could be included to facilitate removal by affinity chromatography during the whole process of VLP purification. Moreover, some other chaperones may replace the function of chaperonin and could potentially have lower interference with the purification of VLP. Therefore, co-expression with those chaperones can be tested in the future, like small heat shock proteins (sHsps)¹⁶⁸.

In conclusion, our results demonstrated the production of recombinant VP3-only VLPs of AAV2 *in situ* in *E. coli* was possible. This required the co-expression of AAP with VP3. In addition, chaperonin was found to further increase the production of VP3-only VLPs when triple co-expression was performed using VP3, AAP and chaperonin. Although the yield of VP3-only VLPs produced in *E. coli* in this project was low compared to VP3-only VLP as reported in other expression systems⁹⁸, we believe this study has demonstrated that there is potential for further investigation and optimization of the process.

REFERENCES

- 1 Mateu, M. G. Virus engineering: functionalization and stabilization. *Protein Eng Des Sel* **24**, 53-63, doi:10.1093/protein/gzq069 (2011).
- 2 Steinmetz, N. F. Viral nanoparticles as platforms for next-generation therapeutics and imaging devices. *Nanomedicine* **6**, 634-641, doi:10.1016/j.nano.2010.04.005 (2010).
- 3 Ding, X., Liu, D., Booth, G., Gao, W. & Lu, Y. Virus-Like Particle Engineering: From Rational Design to Versatile Applications. *Biotechnol J* **13**, e1700324, doi:10.1002/biot.201700324 (2018).
- 4 Nooraei, S. *et al.* Virus-like particles: preparation, immunogenicity and their roles as nanovaccines and drug nanocarriers. *J Nanobiotechnology* **19**, 59, doi:10.1186/s12951-021-00806-7 (2021).
- 5 Tariq, H., Batool, S., Asif, S., Ali, M. & Abbasi, B. H. Virus-Like Particles: Revolutionary Platforms for Developing Vaccines Against Emerging Infectious Diseases. *Front Microbiol* **12**, 790121, doi:10.3389/fmicb.2021.790121 (2021).
- 6 Huang, X., Wang, X., Zhang, J., Xia, N. & Zhao, Q. Escherichia coli-derived virus-like particles in vaccine development. *NPJ Vaccines* **2**, 3, doi:10.1038/s41541-017-0006-8 (2017).

- 7 Choi, J. H., Keum, K. C. & Lee, S. Y. Production of recombinant proteins by high cell density culture of. *Chemical Engineering Science* **61**, 876-885, doi:10.1016/j.ces.2005.03.031 (2006).
- 8 Middelberg, A. P. *et al.* A microbial platform for rapid and low-cost virus-like particle and capsomere vaccines. *Vaccine* **29**, 7154-7162, doi:10.1016/j.vaccine.2011.05.075 (2011).
- 9 Zeltins, A. Construction and characterization of virus-like particles: a review. *Mol Biotechnol* **53**, 92-107, doi:10.1007/s12033-012-9598-4 (2013).
- 10 Vicente, T., Roldao, A., Peixoto, C., Carrondo, M. J. & Alves, P. M. Large-scale production and purification of VLP-based vaccines. *J Invertebr Pathol* **107 Suppl**, S42-48, doi:10.1016/j.jip.2011.05.004 (2011).
- 11 Lai, C. C. *et al.* Process development for pandemic influenza VLP vaccine production using a baculovirus expression system. *J Biol Eng* **13**, 78, doi:10.1186/s13036-019-0206-z (2019).
- 12 Hillebrandt, N., Vormittag, P., Bluthardt, N., Dietrich, A. & Hubbuch, J. Integrated Process for Capture and Purification of Virus-Like Particles: Enhancing Process Performance by Cross-Flow Filtration. *Front Bioeng Biotechnol* **8**, 489, doi:10.3389/fbioe.2020.00489 (2020).
- 13 Pniewski, T. *et al.* Low-dose oral immunization with lyophilized tissue of herbicide-resistant lettuce expressing hepatitis B surface antigen for prototype

- plant-derived vaccine tablet formulation. *J Appl Genet* **52**, 125-136, doi:10.1007/s13353-010-0001-5 (2011).
- 14 Chichester, J. A. *et al.* Safety and immunogenicity of a plant-produced Pfs25 virus-like particle as a transmission blocking vaccine against malaria: A Phase 1 dose-escalation study in healthy adults. *Vaccine* **36**, 5865-5871, doi:10.1016/j.vaccine.2018.08.033 (2018).
- 15 Hutchins, B. *et al.* Working toward an adenoviral vector testing standard. *Mol Ther* **2**, 532-534, doi:10.1006/mthe.2000.0217 (2000).
- 16 Yang, C. *et al.* Hepatitis E virus capsid protein assembles in 4M urea in the presence of salts. *Protein Sci* **22**, 314-326, doi:10.1002/pro.2213 (2013).
- 17 Hickey, J. M. *et al.* Challenges and opportunities of using liquid chromatography and mass spectrometry methods to develop complex vaccine antigens as pharmaceutical dosage forms. *J Chromatogr B Analyt Technol Biomed Life Sci* **1032**, 23-38, doi:10.1016/j.jchromb.2016.04.001 (2016).
- 18 Zhang, X. *et al.* Robust manufacturing and comprehensive characterization of recombinant hepatitis E virus-like particles in Hecolin((R)). *Vaccine* **32**, 4039-4050, doi:10.1016/j.vaccine.2014.05.064 (2014).
- 19 Deschuyteneer, M. *et al.* Molecular and structural characterization of the L1 virus-like particles that are used as vaccine antigens in Cervarix, the AS04-adjuvanted HPV-16 and -18 cervical cancer vaccine. *Hum Vaccin* **6**, 407-419, doi:10.4161/hv.6.5.11023 (2010).

- 20 Zhao, Q. *et al.* Disassembly and reassembly improves morphology and thermal stability of human papillomavirus type 16 virus-like particles. *Nanomedicine* **8**, 1182-1189, doi:10.1016/j.nano.2012.01.007 (2012).
- 21 Shank-Retzlaff, M. L. *et al.* Evaluation of the thermal stability of Gardasil. *Hum Vaccin* **2**, 147-154, doi:10.4161/hv.2.4.2989 (2006).
- 22 Jain, N. K. *et al.* Formulation and stabilization of recombinant protein based virus-like particle vaccines. *Adv Drug Deliv Rev* **93**, 42-55, doi:10.1016/j.addr.2014.10.023 (2015).
- 23 Tleugabulova, D., Falcon, V., Sewer, M. & Penton, E. Aggregation of recombinant hepatitis B surface antigen in *Pichia pastoris*. *J Chromatogr B Biomed Sci Appl* **716**, 209-219, doi:10.1016/s0378-4347(98)00297-7 (1998).
- 24 Tleugabulova, D., Falcon, V. & Penton, E. Physico-chemical characterization of recombinant hepatitis B surface antigen by a multidimensional approach. *J Chromatogr A* **845**, 171-179, doi:10.1016/s0021-9673(99)00009-6 (1999).
- 25 Kee, G. S., Pujar, N. S. & Titchener-Hooker, N. J. Study of detergent-mediated liberation of hepatitis B virus-like particles from *S. cerevisiae* homogenate: identifying a framework for the design of future-generation lipoprotein vaccine processes. *Biotechnol Prog* **24**, 623-631, doi:10.1021/bp070472i (2008).
- 26 Kanno, T. *et al.* Size distribution measurement of vesicles by atomic force microscopy. *Anal Biochem* **309**, 196-199, doi:10.1016/s0003-2697(02)00291-9 (2002).

- 27 Edwards, G. B., Muthurajan, U. M., Bowerman, S. & Luger, K. Analytical Ultracentrifugation (AUC): An Overview of the Application of Fluorescence and Absorbance AUC to the Study of Biological Macromolecules. *Curr Protoc Mol Biol* **133**, e131, doi:10.1002/cpmb.131 (2020).
- 28 Zhang, Y. *et al.* Comparable quality attributes of hepatitis E vaccine antigen with and without adjuvant adsorption-dissolution treatment. *Hum Vaccin Immunother* **11**, 1129-1139, doi:10.1080/21645515.2015.1009343 (2015).
- 29 Zhu, Y. *et al.* Toward the development of monoclonal antibody-based assays to probe virion-like epitopes in hepatitis B vaccine antigen. *Hum Vaccin Immunother* **10**, 1013-1023, doi:10.4161/hv.27753 (2014).
- 30 Riddell, M. A., Li, F. & Anderson, D. A. Identification of immunodominant and conformational epitopes in the capsid protein of hepatitis E virus by using monoclonal antibodies. *J Virol* **74**, 8011-8017, doi:10.1128/jvi.74.17.8011-8017.2000 (2000).
- 31 Mulder, A. M. *et al.* Toolbox for non-intrusive structural and functional analysis of recombinant VLP based vaccines: a case study with hepatitis B vaccine. *PLoS One* **7**, e33235, doi:10.1371/journal.pone.0033235 (2012).
- 32 Zhao, Q. *et al.* Real time monitoring of antigenicity development of HBsAg virus-like particles (VLPs) during heat- and redox-treatment. *Biochem Biophys Res Commun* **408**, 447-453, doi:10.1016/j.bbrc.2011.04.048 (2011).

- 33 Freivalds, J. *et al.* Assembly of bacteriophage Qbeta virus-like particles in yeast *Saccharomyces cerevisiae* and *Pichia pastoris*. *J Biotechnol* **123**, 297-303, doi:10.1016/j.jbiotec.2005.11.013 (2006).
- 34 Li, T. C. *et al.* Characterization of self-assembled virus-like particles of human polyomavirus BK generated by recombinant baculoviruses. *Virology* **311**, 115-124, doi:10.1016/s0042-6822(03)00141-7 (2003).
- 35 White, L. J., Hardy, M. E. & Estes, M. K. Biochemical characterization of a smaller form of recombinant Norwalk virus capsids assembled in insect cells. *J Virol* **71**, 8066-8072, doi:10.1128/JVI.71.10.8066-8072.1997 (1997).
- 36 Venters, C., Graham, W. & Cassidy, W. Recombivax-HB: perspectives past, present and future. *Expert Rev Vaccines* **3**, 119-129, doi:10.1586/14760584.3.2.119 (2004).
- 37 Koutsky, L. The epidemiology behind the HPV vaccine discovery. *Ann Epidemiol* **19**, 239-244, doi:10.1016/j.annepidem.2009.01.023 (2009).
- 38 Schoonen, L. & van Hest, J. C. Functionalization of protein-based nanocages for drug delivery applications. *Nanoscale* **6**, 7124-7141, doi:10.1039/c4nr00915k (2014).
- 39 Rohovie, M. J., Nagasawa, M. & Swartz, J. R. Virus-like particles: Next-generation nanoparticles for targeted therapeutic delivery. *Bioeng Transl Med* **2**, 43-57, doi:10.1002/btm2.10049 (2017).

- 40 Shirbaghaee, Z. & Bolhassani, A. Different applications of virus-like particles in biology and medicine: Vaccination and delivery systems. *Biopolymers* **105**, 113-132, doi:10.1002/bip.22759 (2016).
- 41 Chakraborty, C., Sharma, A. R., Sharma, G., Doss, C. G. P. & Lee, S. S. Therapeutic miRNA and siRNA: Moving from Bench to Clinic as Next Generation Medicine. *Mol Ther Nucleic Acids* **8**, 132-143, doi:10.1016/j.omtn.2017.06.005 (2017).
- 42 Anderson, E. A. *et al.* Viral nanoparticles donning a paramagnetic coat: conjugation of MRI contrast agents to the MS2 capsid. *Nano Lett* **6**, 1160-1164, doi:10.1021/nl060378g (2006).
- 43 Jordan, P. C. *et al.* Self-assembling biomolecular catalysts for hydrogen production. *Nat Chem* **8**, 179-185, doi:10.1038/nchem.2416 (2016).
- 44 Fiedler, J. D., Brown, S. D., Lau, J. L. & Finn, M. G. RNA-directed packaging of enzymes within virus-like particles. *Angew Chem Int Ed Engl* **49**, 9648-9651, doi:10.1002/anie.201005243 (2010).
- 45 Comellas-Aragones, M. *et al.* A virus-based single-enzyme nanoreactor. *Nat Nanotechnol* **2**, 635-639, doi:10.1038/nnano.2007.299 (2007).
- 46 Lyu, P., Wang, L. & Lu, B. Virus-Like Particle Mediated CRISPR/Cas9 Delivery for Efficient and Safe Genome Editing. *Life (Basel)* **10**, doi:10.3390/life10120366 (2020).

- 47 Wang, D., Tai, P. W. L. & Gao, G. Adeno-associated virus vector as a platform for gene therapy delivery. *Nat Rev Drug Discov* **18**, 358-378, doi:10.1038/s41573-019-0012-9 (2019).
- 48 Meier, A. F., Fraefel, C. & Seyffert, M. The Interplay between Adeno-Associated Virus and its Helper Viruses. *Viruses* **12**, doi:10.3390/v12060662 (2020).
- 49 Atchison, R. W., Casto, B. C. & Hammon, W. M. Adenovirus-Associated Defective Virus Particles. *Science* **149**, 754-756, doi:10.1126/science.149.3685.754 (1965).
- 50 Hoggan, M. D., Blacklow, N. R. & Rowe, W. P. Studies of small DNA viruses found in various adenovirus preparations: physical, biological, and immunological characteristics. *Proc Natl Acad Sci U S A* **55**, 1467-1474, doi:10.1073/pnas.55.6.1467 (1966).
- 51 Blacklow, N. R., Hoggan, M. D. & Rowe, W. P. Isolation of adenovirus-associated viruses from man. *Proc Natl Acad Sci U S A* **58**, 1410-1415, doi:10.1073/pnas.58.4.1410 (1967).
- 52 Wu, Z., Yang, H. & Colosi, P. Effect of genome size on AAV vector packaging. *Mol Ther* **18**, 80-86, doi:10.1038/mt.2009.255 (2010).
- 53 Carter, B. J. Adeno-associated virus and the development of adeno-associated virus vectors: a historical perspective. *Mol Ther* **10**, 981-989, doi:10.1016/j.ymthe.2004.09.011 (2004).

- 54 Wu, Z. J., Asokan, A. & Samulski, R. J. Adeno-associated virus serotypes: Vector toolkit for human gene therapy. *Molecular Therapy* **14**, 316-327, doi:10.1016/j.ymthe.2006.05.009 (2006).
- 55 Bennett, A., Mietzsch, M. & Agbandje-McKenna, M. Understanding capsid assembly and genome packaging for adeno-associated viruses. *Future Virology* **12**, 283-297, doi:10.2217/fvl-2017-0011 (2017).
- 56 Daya, S. & Berns, K. I. Gene therapy using adeno-associated virus vectors. *Clin Microbiol Rev* **21**, 583-593, doi:10.1128/CMR.00008-08 (2008).
- 57 Pereira, D. J., McCarty, D. M. & Muzyczka, N. The adeno-associated virus (AAV) Rep protein acts as both a repressor and an activator to regulate AAV transcription during a productive infection. *J Virol* **71**, 1079-1088, doi:10.1128/JVI.71.2.1079-1088.1997 (1997).
- 58 Girod, A. *et al.* The VP1 capsid protein of adeno-associated virus type 2 is carrying a phospholipase A2 domain required for virus infectivity. *J Gen Virol* **83**, 973-978, doi:10.1099/0022-1317-83-5-973 (2002).
- 59 Sonntag, F., Bleker, S., Leuchs, B., Fischer, R. & Kleinschmidt, J. A. Adeno-associated virus type 2 capsids with externalized VP1/VP2 trafficking domains are generated prior to passage through the cytoplasm and are maintained until uncoating occurs in the nucleus. *J Virol* **80**, 11040-11054, doi:10.1128/JVI.01056-06 (2006).

- 60 Sonntag, F., Schmidt, K. & Kleinschmidt, J. A. A viral assembly factor promotes AAV2 capsid formation in the nucleolus. *Proc Natl Acad Sci U S A* **107**, 10220-10225, doi:10.1073/pnas.1001673107 (2010).
- 61 Kotin, R. M. *et al.* Site-specific integration by adeno-associated virus. *Proc Natl Acad Sci U S A* **87**, 2211-2215, doi:10.1073/pnas.87.6.2211 (1990).
- 62 Surosky, R. T. *et al.* Adeno-associated virus Rep proteins target DNA sequences to a unique locus in the human genome. *J Virol* **71**, 7951-7959, doi:10.1128/JVI.71.10.7951-7959.1997 (1997).
- 63 Colella, P., Ronzitti, G. & Mingozzi, F. Emerging Issues in AAV-Mediated In Vivo Gene Therapy. *Mol Ther Methods Clin Dev* **8**, 87-104, doi:10.1016/j.omtm.2017.11.007 (2018).
- 64 Buller, R. M. & Rose, J. A. Characterization of adenovirus-associated virus-induced polypeptides in KB cells. *J Virol* **25**, 331-338, doi:10.1128/JVI.25.1.331-338.1978 (1978).
- 65 Chapman, M. S. & Rossmann, M. G. Structure, sequence, and function correlations among parvoviruses. *Virology* **194**, 491-508, doi:10.1006/viro.1993.1288 (1993).
- 66 Worner, T. P. *et al.* Adeno-associated virus capsid assembly is divergent and stochastic. *Nat Commun* **12**, 1642, doi:10.1038/s41467-021-21935-5 (2021).

- 67 Xie, Q., Lerch, T. F., Meyer, N. L. & Chapman, M. S. Structure-function analysis of receptor-binding in adeno-associated virus serotype 6 (AAV-6). *Virology* **420**, 10-19, doi:10.1016/j.virol.2011.08.011 (2011).
- 68 Lerch, T. F., Xie, Q. & Chapman, M. S. The structure of adeno-associated virus serotype 3B (AAV-3B): insights into receptor binding and immune evasion. *Virology* **403**, 26-36, doi:10.1016/j.virol.2010.03.027 (2010).
- 69 Ng, R. *et al.* Structural characterization of the dual glycan binding adeno-associated virus serotype 6. *J Virol* **84**, 12945-12957, doi:10.1128/JVI.01235-10 (2010).
- 70 DiMattia, M. A. *et al.* Structural insight into the unique properties of adeno-associated virus serotype 9. *J Virol* **86**, 6947-6958, doi:10.1128/JVI.07232-11 (2012).
- 71 Govindasamy, L. *et al.* Structural insights into adeno-associated virus serotype 5. *J Virol* **87**, 11187-11199, doi:10.1128/JVI.00867-13 (2013).
- 72 Mikals, K. *et al.* The structure of AAVrh32.33, a novel gene delivery vector. *J Struct Biol* **186**, 308-317, doi:10.1016/j.jsb.2014.03.020 (2014).
- 73 Venkatakrishnan, B. *et al.* Structure and dynamics of adeno-associated virus serotype 1 VP1-unique N-terminal domain and its role in capsid trafficking. *J Virol* **87**, 4974-4984, doi:10.1128/JVI.02524-12 (2013).
- 74 Mietzsch, M., Penzes, J. J. & Agbandje-McKenna, M. Twenty-Five Years of Structural Parvovirology. *Viruses* **11**, doi:10.3390/v11040362 (2019).

- 75 Kronenberg, S., Bottcher, B., von der Lieth, C. W., Bleker, S. & Kleinschmidt, J. A. A conformational change in the adeno-associated virus type 2 capsid leads to the exposure of hidden VP1 N termini. *J Virol* **79**, 5296-5303, doi:10.1128/JVI.79.9.5296-5303.2005 (2005).
- 76 Myers, M. W. & Carter, B. J. Assembly of adeno-associated virus. *Virology* **102**, 71-82, doi:10.1016/0042-6822(80)90071-9 (1980).
- 77 Wistuba, A., Kern, A., Weger, S., Grimm, D. & Kleinschmidt, J. A. Subcellular compartmentalization of adeno-associated virus type 2 assembly. *J Virol* **71**, 1341-1352, doi:10.1128/JVI.71.2.1341-1352.1997 (1997).
- 78 Wistuba, A., Weger, S., Kern, A. & Kleinschmidt, J. A. Intermediates of adeno-associated virus type 2 assembly: identification of soluble complexes containing Rep and Cap proteins. *J Virol* **69**, 5311-5319, doi:10.1128/JVI.69.9.5311-5319.1995 (1995).
- 79 Zhang, R. *et al.* Adeno-associated virus 2 bound to its cellular receptor AAVR. *Nat Microbiol* **4**, 675-682, doi:10.1038/s41564-018-0356-7 (2019).
- 80 Ruffing, M., Zentgraf, H. & Kleinschmidt, J. A. Assembly of viruslike particles by recombinant structural proteins of adeno-associated virus type 2 in insect cells. *J Virol* **66**, 6922-6930, doi:10.1128/JVI.66.12.6922-6930.1992 (1992).
- 81 Steinbach, S., Wistuba, A., Bock, T. & Kleinschmidt, J. A. Assembly of adeno-associated virus type 2 capsids in vitro. *J Gen Virol* **78 (Pt 6)**, 1453-1462, doi:10.1099/0022-1317-78-6-1453 (1997).

- 82 Rabinowitz, J. E., Xiao, W. & Samulski, R. J. Insertional mutagenesis of AAV2 capsid and the production of recombinant virus. *Virology* **265**, 274-285, doi:10.1006/viro.1999.0045 (1999).
- 83 Warrington, K. H., Jr. *et al.* Adeno-associated virus type 2 VP2 capsid protein is nonessential and can tolerate large peptide insertions at its N terminus. *J Virol* **78**, 6595-6609, doi:10.1128/JVI.78.12.6595-6609.2004 (2004).
- 84 Grosse, S. *et al.* Relevance of Assembly-Activating Protein for Adeno-associated Virus Vector Production and Capsid Protein Stability in Mammalian and Insect Cells. *J Virol* **91**, doi:10.1128/JVI.01198-17 (2017).
- 85 Earley, L. F. *et al.* Adeno-associated virus assembly-activating protein is not an essential requirement for capsid assembly of AAV serotypes 4, 5 and 11. *Journal of virology*, JVI. 01980-01916 (2016).
- 86 Clark, K. R., Voulgaropoulou, F., Fraley, D. M. & Johnson, P. R. Cell lines for the production of recombinant adeno-associated virus. *Hum Gene Ther* **6**, 1329-1341, doi:10.1089/hum.1995.6.10-1329 (1995).
- 87 Robert, M. A. *et al.* Manufacturing of recombinant adeno-associated viruses using mammalian expression platforms. *Biotechnol J* **12**, doi:10.1002/biot.201600193 (2017).
- 88 Tang, Q. *et al.* Two-Plasmid Packaging System for Recombinant Adeno-Associated Virus. *Biores Open Access* **9**, 219-228, doi:10.1089/biores.2020.0031 (2020).

- 89 Pupo, A. *et al.* AAV vectors: The Rubik's cube of human gene therapy. *Mol Ther* **30**, 3515-3541, doi:10.1016/j.ymthe.2022.09.015 (2022).
- 90 Grieger, J. C., Soltys, S. M. & Samulski, R. J. Production of Recombinant Adeno-associated Virus Vectors Using Suspension HEK293 Cells and Continuous Harvest of Vector From the Culture Media for GMP FIX and FLT1 Clinical Vector. *Mol Ther* **24**, 287-297, doi:10.1038/mt.2015.187 (2016).
- 91 Chadeuf, G., Ciron, C., Moullier, P. & Salvetti, A. Evidence for encapsidation of prokaryotic sequences during recombinant adeno-associated virus production and their in vivo persistence after vector delivery. *Mol Ther* **12**, 744-753, doi:10.1016/j.ymthe.2005.06.003 (2005).
- 92 Hauck, B. *et al.* Undetectable transcription of cap in a clinical AAV vector: implications for preformed capsid in immune responses. *Mol Ther* **17**, 144-152, doi:10.1038/mt.2008.227 (2009).
- 93 Clement, N., Knop, D. R. & Byrne, B. J. Large-scale adeno-associated viral vector production using a herpesvirus-based system enables manufacturing for clinical studies. *Hum Gene Ther* **20**, 796-806, doi:10.1089/hum.2009.094 (2009).
- 94 Thomas, D. L. *et al.* Scalable recombinant adeno-associated virus production using recombinant herpes simplex virus type 1 coinfection of suspension-adapted mammalian cells. *Hum Gene Ther* **20**, 861-870, doi:10.1089/hum.2009.004 (2009).

- 95 Adamson-Small, L., Potter, M., Byrne, B. J. & Clement, N. Sodium Chloride Enhances Recombinant Adeno-Associated Virus Production in a Serum-Free Suspension Manufacturing Platform Using the Herpes Simplex Virus System. *Hum Gene Ther Methods* **28**, 1-14, doi:10.1089/hgtb.2016.151 (2017).
- 96 Urabe, M., Ding, C. & Kotin, R. M. Insect cells as a factory to produce adeno-associated virus type 2 vectors. *Hum Gene Ther* **13**, 1935-1943, doi:10.1089/10430340260355347 (2002).
- 97 Cecchini, S., Virag, T. & Kotin, R. M. Reproducible high yields of recombinant adeno-associated virus produced using invertebrate cells in 0.02- to 200-liter cultures. *Hum Gene Ther* **22**, 1021-1030, doi:10.1089/hum.2010.250 (2011).
- 98 Kotin, R. M. Large-scale recombinant adeno-associated virus production. *Hum Mol Genet* **20**, R2-6, doi:10.1093/hmg/ddr141 (2011).
- 99 Rumachik, N. G. *et al.* Methods Matter: Standard Production Platforms for Recombinant AAV Produce Chemically and Functionally Distinct Vectors. *Mol Ther Methods Clin Dev* **18**, 98-118, doi:10.1016/j.omtm.2020.05.018 (2020).
- 100 Backovic, A. *et al.* Capsid protein expression and adeno-associated virus like particles assembly in *Saccharomyces cerevisiae*. *Microb Cell Fact* **11**, 124, doi:10.1186/1475-2859-11-124 (2012).
- 101 Le, D. T., Radukic, M. T., Teschner, K., Becker, L. & Muller, K. M. Synthesis and Concomitant Assembly of Adeno-Associated Virus-like Particles in *Escherichia coli*. *ACS Synth Biol* **11**, 3601-3607, doi:10.1021/acssynbio.2c00451 (2022).

- 102 Le, D. T., Radukic, M. T. & Muller, K. M. Adeno-associated virus capsid protein expression in *Escherichia coli* and chemically defined capsid assembly. *Sci Rep* **9**, 18631, doi:10.1038/s41598-019-54928-y (2019).
- 103 Le, D. T. & Muller, K. M. In Vitro Assembly of Virus-Like Particles and Their Applications. *Life (Basel)* **11**, doi:10.3390/life11040334 (2021).
- 104 Meselson, M., Stahl, F. W. & Vinograd, J. Equilibrium Sedimentation of Macromolecules in Density Gradients. *Proc Natl Acad Sci U S A* **43**, 581-588, doi:10.1073/pnas.43.7.581 (1957).
- 105 Belova, L., Kochergin-Nikitsky, K., Erofeeva, A., Lavrov, A. & Smirnikhina, S. Approaches to purification and concentration of rAAV vectors for gene therapy. *Bioessays* **44**, e2200019, doi:10.1002/bies.202200019 (2022).
- 106 de la Maza, L. M. & Carter, B. J. Heavy and light particles of adeno-associated virus. *J Virol* **33**, 1129-1137, doi:10.1128/JVI.33.3.1129-1137.1980 (1980).
- 107 Strobel, B., Miller, F. D., Rist, W. & Lamla, T. Comparative Analysis of Cesium Chloride- and Iodixanol-Based Purification of Recombinant Adeno-Associated Viral Vectors for Preclinical Applications. *Hum Gene Ther Methods* **26**, 147-157, doi:10.1089/hgtb.2015.051 (2015).
- 108 Grieger, J. C., Choi, V. W. & Samulski, R. J. Production and characterization of adeno-associated viral vectors. *Nature protocols* **1**, 1412-1428, doi:10.1038/nprot.2006.207 (2006).

- 109 Zolotukhin, S. *et al.* Recombinant adeno-associated virus purification using novel methods improves infectious titer and yield. *Gene Therapy* **6**, 973-985, doi:DOI 10.1038/sj.gt.3300938 (1999).
- 110 Nagrath, D., Xia, F. & Cramer, S. M. Characterization and modeling of nonlinear hydrophobic interaction chromatographic systems. *J Chromatogr A* **1218**, 1219-1226, doi:10.1016/j.chroma.2010.12.111 (2011).
- 111 Melander, W. R., Corradini, D. & Horvath, C. Salt-mediated retention of proteins in hydrophobic-interaction chromatography. Application of solvophobic theory. *J Chromatogr* **317**, 67-85, doi:10.1016/s0021-9673(01)91648-6 (1984).
- 112 Qu, W., Wang, M., Wu, Y. & Xu, R. Scalable downstream strategies for purification of recombinant adeno-associated virus vectors in light of the properties. *Curr Pharm Biotechnol* **16**, 684-695, doi:10.2174/1389201016666150505122228 (2015).
- 113 McNally, D. J., Piras, B. A., Willis, C. M., Lockey, T. D. & Meagher, M. M. Development and Optimization of a Hydrophobic Interaction Chromatography-Based Method of AAV Harvest, Capture, and Recovery. *Mol Ther Methods Clin Dev* **19**, 275-284, doi:10.1016/j.omtm.2020.09.015 (2020).
- 114 Burova, E. & Ioffe, E. Chromatographic purification of recombinant adenoviral and adeno-associated viral vectors: methods and implications. *Gene Ther* **12 Suppl 1**, S5-17, doi:10.1038/sj.gt.3302611 (2005).

- 115 Davidoff, A. M. *et al.* Purification of recombinant adeno-associated virus type 8 vectors by ion exchange chromatography generates clinical grade vector stock. *J Virol Methods* **121**, 209-215, doi:10.1016/j.jviromet.2004.07.001 (2004).
- 116 McIntosh, N. L. *et al.* Comprehensive characterization and quantification of adeno associated vectors by size exclusion chromatography and multi angle light scattering. *Sci Rep* **11**, 3012, doi:10.1038/s41598-021-82599-1 (2021).
- 117 Sahin, E. & Roberts, C. J. Size-exclusion chromatography with multi-angle light scattering for elucidating protein aggregation mechanisms. *Methods Mol Biol* **899**, 403-423, doi:10.1007/978-1-61779-921-1_25 (2012).
- 118 Smith, R. H., Yang, L. & Kotin, R. M. Chromatography-based purification of adeno-associated virus. *Methods Mol Biol* **434**, 37-54, doi:10.1007/978-1-60327-248-3_4 (2008).
- 119 Urabe, M. *et al.* Removal of empty capsids from type 1 adeno-associated virus vector stocks by anion-exchange chromatography potentiates transgene expression. *Mol Ther* **13**, 823-828, doi:10.1016/j.ymthe.2005.11.024 (2006).
- 120 Tomono, T. *et al.* Ultracentrifugation-free chromatography-mediated large-scale purification of recombinant adeno-associated virus serotype 1 (rAAV1). *Mol Ther Methods Clin Dev* **3**, 15058, doi:10.1038/mtm.2015.58 (2016).
- 121 Miyake, K., Miyake, N., Yamazaki, Y., Shimada, T. & Hirai, Y. Serotype-independent method of recombinant adeno-associated virus (AAV) vector

- production and purification. *J Nippon Med Sch* **79**, 394-402, doi:10.1272/jnms.79.394 (2012).
- 122 Smith, R. H., Ding, C. & Kotin, R. M. Serum-free production and column purification of adeno-associated virus type 5. *J Virol Methods* **114**, 115-124, doi:10.1016/j.jviromet.2003.09.002 (2003).
- 123 Allay, J. A. *et al.* Good manufacturing practice production of self-complementary serotype 8 adeno-associated viral vector for a hemophilia B clinical trial. *Hum Gene Ther* **22**, 595-604, doi:10.1089/hum.2010.202 (2011).
- 124 Tomono, T. *et al.* Highly Efficient Ultracentrifugation-free Chromatographic Purification of Recombinant AAV Serotype 9. *Mol Ther Methods Clin Dev* **11**, 180-190, doi:10.1016/j.omtm.2018.10.015 (2018).
- 125 van Lieshout, L. P. *et al.* Engineered AAV8 capsid acquires heparin and AVB sepharose binding capacity but has altered in vivo transduction efficiency. *Gene Ther* **30**, 236-244, doi:10.1038/s41434-020-00198-7 (2023).
- 126 Opie, S. R., Warrington, K. H., Jr., Agbandje-McKenna, M., Zolotukhin, S. & Muzyczka, N. Identification of amino acid residues in the capsid proteins of adeno-associated virus type 2 that contribute to heparan sulfate proteoglycan binding. *J Virol* **77**, 6995-7006, doi:10.1128/jvi.77.12.6995-7006.2003 (2003).
- 127 Auricchio, A., Sena-Esteves, M. & Gao, G. Purification of Recombinant Adeno-Associated Virus 2 (rAAV2) by Heparin Column Affinity Chromatography. *Cold Spring Harb Protoc* **2020**, 095620, doi:10.1101/pdb.prot095620 (2020).

- 128 Wu, Z. *et al.* Single amino acid changes can influence titer, heparin binding, and tissue tropism in different adeno-associated virus serotypes. *J Virol* **80**, 11393-11397, doi:10.1128/JVI.01288-06 (2006).
- 129 Mietzsch, M. *et al.* Characterization of AAV-Specific Affinity Ligands: Consequences for Vector Purification and Development Strategies. *Mol Ther Methods Clin Dev* **19**, 362-373, doi:10.1016/j.omtm.2020.10.001 (2020).
- 130 Nass, S. A. *et al.* Universal Method for the Purification of Recombinant AAV Vectors of Differing Serotypes. *Mol Ther Methods Clin Dev* **9**, 33-46, doi:10.1016/j.omtm.2017.12.004 (2018).
- 131 Florea, M. *et al.* High-efficiency purification of divergent AAV serotypes using AAVX affinity chromatography. *Mol Ther Methods Clin Dev* **28**, 146-159, doi:10.1016/j.omtm.2022.12.009 (2023).
- 132 de Marco, A., Deuerling, E., Mogk, A., Tomoyasu, T. & Bukau, B. Chaperone-based procedure to increase yields of soluble recombinant proteins produced in *E. coli*. *BMC Biotechnol* **7**, 32, doi:10.1186/1472-6750-7-32 (2007).
- 133 Schlieker, C., Bukau, B. & Mogk, A. Prevention and reversion of protein aggregation by molecular chaperones in the *E. coli* cytosol: implications for their applicability in biotechnology. *J Biotechnol* **96**, 13-21, doi:10.1016/s0168-1656(02)00033-0 (2002).

- 134 Fatima, K., Naqvi, F. & Younas, H. A Review: Molecular Chaperone-mediated Folding, Unfolding and Disaggregation of Expressed Recombinant Proteins. *Cell Biochem Biophys* **79**, 153-174, doi:10.1007/s12013-021-00970-5 (2021).
- 135 Buchner, J. *et al.* GroE facilitates refolding of citrate synthase by suppressing aggregation. *Biochemistry* **30**, 1586-1591, doi:10.1021/bi00220a020 (1991).
- 136 Schroder, H., Langer, T., Hartl, F. U. & Bukau, B. DnaK, DnaJ and GrpE form a cellular chaperone machinery capable of repairing heat-induced protein damage. *EMBO J* **12**, 4137-4144, doi:10.1002/j.1460-2075.1993.tb06097.x (1993).
- 137 Goloubinoff, P., Mogk, A., Zvi, A. P., Tomoyasu, T. & Bukau, B. Sequential mechanism of solubilization and refolding of stable protein aggregates by a bichaperone network. *Proc Natl Acad Sci U S A* **96**, 13732-13737, doi:10.1073/pnas.96.24.13732 (1999).
- 138 Mogk, A. *et al.* Identification of thermolabile Escherichia coli proteins: prevention and reversion of aggregation by DnaK and ClpB. *EMBO J* **18**, 6934-6949, doi:10.1093/emboj/18.24.6934 (1999).
- 139 Watanabe, Y. H., Motohashi, K., Taguchi, H. & Yoshida, M. Heat-inactivated proteins managed by DnaKJ-GrpE-ClpB chaperones are released as a chaperonin-recognizable non-native form. *J Biol Chem* **275**, 12388-12392, doi:10.1074/jbc.275.17.12388 (2000).
- 140 Kiefhaber, T., Rudolph, R., Kohler, H. H. & Buchner, J. Protein aggregation in vitro and in vivo: a quantitative model of the kinetic competition between folding

- and aggregation. *Biotechnology (N Y)* **9**, 825-829, doi:10.1038/nbt0991-825 (1991).
- 141 King, J. & Betts, S. A green light for protein folding. *Nat Biotechnol* **17**, 637-638, doi:10.1038/10848 (1999).
- 142 Schrodell, A. & de Marco, A. Characterization of the aggregates formed during recombinant protein expression in bacteria. *BMC Biochem* **6**, 10, doi:10.1186/1471-2091-6-10 (2005).
- 143 Amrein, K. E. *et al.* Purification and characterization of recombinant human p50^{cas} protein-tyrosine kinase from an Escherichia coli expression system overproducing the bacterial chaperones GroES and GroEL. *Proc Natl Acad Sci U S A* **92**, 1048-1052, doi:10.1073/pnas.92.4.1048 (1995).
- 144 Dale, G. E., Schonfeld, H. J., Langen, H. & Stieger, M. Increased solubility of trimethoprim-resistant type S1 DHFR from Staphylococcus aureus in Escherichia coli cells overproducing the chaperonins GroEL and GroES. *Protein Eng* **7**, 925-931, doi:10.1093/protein/7.7.925 (1994).
- 145 de Marco, A., Volrath, S., Bruyere, T., Law, M. & Fonne-Pfister, R. Recombinant maize protoporphyrinogen IX oxidase expressed in Escherichia coli forms complexes with GroEL and DnaK chaperones. *Protein Expr Purif* **20**, 81-86, doi:10.1006/pep.2000.1274 (2000).
- 146 O'Prey, J. *et al.* Application of CRISPR/Cas9 to Autophagy Research. *Methods Enzymol* **588**, 79-108, doi:10.1016/bs.mie.2016.09.076 (2017).

- 147 Motoshashi, K. in *In Vitro Mutagenesis Methods in Molecular Biology* Ch. Chapter 23, 349-357 (2017).
- 148 Zhang, Y., Werling, U. & Edelmann, W. Seamless Ligation Cloning Extract (SLiCE) cloning method. *Methods Mol Biol* **1116**, 235-244, doi:10.1007/978-1-62703-764-8_16 (2014).
- 149 Studier, F. W. Protein production by auto-induction in high density shaking cultures. *Protein Expr Purif* **41**, 207-234, doi:10.1016/j.pep.2005.01.016 (2005).
- 150 Faust, G., Stand, A. & Weuster-Botz, D. IPTG can replace lactose in auto-induction media to enhance protein expression in batch-cultured *Escherichia coli*. *Engineering in Life Sciences* **15**, 824-829, doi:10.1002/elsc.201500011 (2015).
- 151 Brunelle, J. L. & Green, R. Coomassie blue staining. *Methods Enzymol* **541**, 161-167, doi:10.1016/B978-0-12-420119-4.00013-6 (2014).
- 152 Challis, R. C. *et al.* Systemic AAV vectors for widespread and targeted gene delivery in rodents. *Nature protocols* **14**, 379-414, doi:10.1038/s41596-018-0097-3 (2019).
- 153 Aida, Y. & Pabst, M. J. Removal of endotoxin from protein solutions by phase separation using Triton X-114. *J Immunol Methods* **132**, 191-195, doi:10.1016/0022-1759(90)90029-u (1990).
- 154 Burgess, R. R. in *Guide to Protein Purification, 2nd Edition Methods in Enzymology* 331-342 (2009).

- 155 Maurer, A. C. *et al.* The Assembly-Activating Protein Promotes Stability and Interactions between AAV's Viral Proteins to Nucleate Capsid Assembly. *Cell Rep* **23**, 1817-1830, doi:10.1016/j.celrep.2018.04.026 (2018).
- 156 Wobus, C. E. *et al.* Monoclonal antibodies against the adeno-associated virus type 2 (AAV-2) capsid: epitope mapping and identification of capsid domains involved in AAV-2-cell interaction and neutralization of AAV-2 infection. *J Virol* **74**, 9281-9293, doi:10.1128/jvi.74.19.9281-9293.2000 (2000).
- 157 Chahal, P. S., Aucoin, M. G. & Kamen, A. Primary recovery and chromatographic purification of adeno-associated virus type 2 produced by baculovirus/insect cell system. *J Virol Methods* **139**, 61-70, doi:10.1016/j.jviromet.2006.09.011 (2007).
- 158 Wright, J. F. *et al.* Identification of factors that contribute to recombinant AAV2 particle aggregation and methods to prevent its occurrence during vector purification and formulation. *Mol Ther* **12**, 171-178, doi:10.1016/j.ymthe.2005.02.021 (2005).
- 159 Kondratova, L., Kondratov, O., Ragheb, R. & Zolotukhin, S. Removal of Endotoxin from rAAV Samples Using a Simple Detergent-Based Protocol. *Mol Ther Methods Clin Dev* **15**, 112-119, doi:10.1016/j.omtm.2019.08.013 (2019).
- 160 Adams, B., Bak, H. & Tustian, A. D. Moving from the bench towards a large scale, industrial platform process for adeno-associated viral vector purification. *Biotechnol Bioeng* **117**, 3199-3211, doi:10.1002/bit.27472 (2020).

- 161 Gorovits, B. M. & Horowitz, P. M. The chaperonin GroEL is destabilized by binding of ADP. *J Biol Chem* **270**, 28551-28556, doi:10.1074/jbc.270.48.28551 (1995).
- 162 Lissin, N. M. In vitro dissociation of self-assembly of three chaperonin 60s: the role of ATP. *FEBS Lett* **361**, 55-60, doi:10.1016/0014-5793(95)00151-x (1995).
- 163 Vandenberghe, L. H., Wilson, J. M. & Gao, G. Tailoring the AAV vector capsid for gene therapy. *Gene Ther* **16**, 311-319, doi:10.1038/gt.2008.170 (2009).
- 164 Rosano, G. L. & Ceccarelli, E. A. Recombinant protein expression in Escherichia coli: advances and challenges. *Front Microbiol* **5**, 172, doi:10.3389/fmicb.2014.00172 (2014).
- 165 Hagan, M. F. Modeling Viral Capsid Assembly. *Adv Chem Phys* **155**, 1-68, doi:10.1002/9781118755815.ch01 (2014).
- 166 Earley, L. F. *et al.* Adeno-associated Virus (AAV) Assembly-Activating Protein Is Not an Essential Requirement for Capsid Assembly of AAV Serotypes 4, 5, and 11. *Journal of Virology* **91**, doi:10.1128/jvi.01980-16 (2017).
- 167 Kaufmann, B., Simpson, A. A. & Rossmann, M. G. The structure of human parvovirus B19. *Proceedings of the National Academy of Sciences* **101**, 11628-11633, doi:10.1073/pnas.0402992101 (2004).
- 168 Obuchowski, I., Karas, P. & Liberek, K. The Small Ones Matter-sHsps in the Bacterial Chaperone Network. *Front Mol Biosci* **8**, 666893, doi:10.3389/fmolb.2021.666893 (2021).

Vita

Name	<i>Chengyu Fu</i>
Baccalaureate Degree	<i>Bachelor of Science, China Pharmaceutical University, Nanjing, Major: Pharmacy</i>
Date Graduated	<i>June, 2014</i>
Other Degrees and Certificates	<i>Master of Science, China Pharmaceutical University, Nanjing Major: Pharmacology</i>
Date Graduated	<i>May, 2017</i>